

Temporal spike pattern learningSachin S. Talathi,^{1,*} Henry D. I. Abarbanel,² and William L. Ditto¹¹*J. Crayton Pruitt Family Department of Biomedical Engineering, University of Florida, Florida 32611, USA*²*Marine Physical Laboratory, Scripps Institution of Oceanography, Department of Physics and Center for Theoretical Biological Physics, University of California, San Diego, La Jolla, California 92093, USA*

(Received 16 June 2008; revised manuscript received 11 August 2008; published 23 September 2008)

Sensory systems pass information about an animal's environment to higher nervous system units through sequences of action potentials. When these action potentials have essentially equivalent wave forms, all information is contained in the interspike intervals (ISIs) of the spike sequence. How do neural circuits recognize and read these ISI sequences? We address this issue of temporal sequence learning by a neuronal system utilizing spike timing dependent plasticity (STDP). We present a general architecture of neural circuitry that can perform the task of ISI recognition. The essential ingredients of this neural circuit, which we refer to as "interspike interval recognition unit" (IRU) are (i) a spike selection unit, the function of which is to selectively distribute input spikes to downstream IRU circuitry; (ii) a time-delay unit that can be tuned by STDP; and (iii) a detection unit, which is the output of the IRU and a spike from which indicates successful ISI recognition by the IRU. We present two distinct configurations for the time-delay circuit within the IRU using excitatory and inhibitory synapses, respectively, to produce a delayed output spike at time $t_0 + \tau(R)$ in response to the input spike received at time t_0 . R is the tunable parameter of the time-delay circuit that controls the timing of the delayed output spike. We discuss the forms of STDP rules for excitatory and inhibitory synapses, respectively, that allow for modulation of R for the IRU to perform its task of ISI recognition. We then present two specific implementations for the IRU circuitry, derived from the general architecture that can both learn the ISIs of a training sequence and then recognize the same ISI sequence when it is presented on subsequent occasions.

DOI: [10.1103/PhysRevE.78.031918](https://doi.org/10.1103/PhysRevE.78.031918)

PACS number(s): 87.19.lj, 87.19.1l, 87.19.lw, 87.18.Sn

I. INTRODUCTION

Sensory systems transform environmental analog signals into a format composed of essentially identical action potentials. These are sent for further processing to other areas of the central nervous system. When the action potentials or spikes are comprised of identical wave forms all information about the environment is contained in the intervals between spike arrival times [1]. There are many examples of sensitive stimulus-response properties characterizing how neurons respond to specific stimuli. These include whisker-selective neural response in barrel cortex [2,3] of rats and motion sensitive cells in the visual cortical areas of the primates [4,5].

One striking example is the selective auditory response of neurons in the songbird telencephalic nucleus HVC (used as a proper name) [6–9]. Projection neurons within HVC fire sparse bursts of spikes when presented with auditory playback of the bird's own song (BOS) and are quite unresponsive to other auditory inputs. Nucleus NIf (interfacial nucleus of nidopallium), through which auditory signals reach HVC [6,10–12], also strongly responds to BOS in addition to responding to a broad range of other auditory stimuli. NIf projects to HVC, and the similarity of NIf responses to the auditory input and the subthreshold activity in HVC neurons suggests that NIf could be acting as a nonlinear filter for BOS, preferentially passing that important signal on to HVC.

It was these examples from birdsong that led us to address the interspike interval (ISI) reading problem. Based on ob-

served neural circuitry in the songbird brain, we proposed [13] a neural circuit comprised of inhibitory synapses, that can train itself to respond to a given temporal sequence of input spikes using spike timing dependent plasticity (STDP) of inhibitory synapses [14]. In this paper we consider the general problem of ISI recognition and elaborate the key ingredients essential to any neural circuitry assigned the task of ISI recognition. We demonstrate how biologically realistic neurons and synapses can be used to construct and train such a network to decode the temporal information in the input spike pattern. We call the resulting networks, an ISI reading unit (IRU). It should be noted that by "decoding" we mean the recognition of a specific ISI sequence on which the network was trained in preference to any other ISI sequence.

Key to the functioning of an IRU are two biological processes:

(1) A time-delay unit which produces an output spike at time $t_0 + \tau(R)$ in response to an input spike at time t_0 . R is a dimensionless parameter characterizing the strength of a synapse within the time-delay circuit that can be used to tune the time delay $\tau(R)$.

(2) A method for tuning the time delays $\tau(R)$ in the IRU using observed synaptic plasticity rules [14–16].

Time-delay circuits, thought of primarily as an abstract idea rather than as a particular biological circuit realization, have been considered before [17–19]. One exception to the descriptive modeling of neural time keeping processes is the work of Buonomano [20] which studies a two neuron model that can be tuned to respond to time delays. Buonomano identifies synaptic changes as the tuning mechanism that might underlie detection of time intervals. His model relies on a balance between excitatory and inhibitory synaptic

*stalathi@bme.ufl.edu

strengths. We do not explore the scheme proposed by Buonomano here; instead we present an alternative general scheme to decode the ISI signal.

As discussed by earlier authors, circuits for marking time more or less divide into three categories:

(1) Time delays along pieces of axon resulting in delays as short as a few microseconds. These are found in detection circuits for interaural time differences [11,21–23];

(2) Time delays of order hours or days connected with circadian rhythms. A detailed model of the biochemical processes thought to underly the ≈ 24 h circadian rhythm is found in recent work by Forger and Peskin [24,25], where a limit cycle oscillator with a period slightly more than 24 h is identified and analyzed.

(3) Time delays of tens to hundreds of milliseconds associated with cortical and other neural processing [26].

Our realization of the time-delay circuit addresses this third category of time keeping.

In investigating time differences between signals propagating from the birdsong nucleus HVC directly to the premotor nucleus RA (robust nucleus of acropallium) and the same signal propagating to RA around the neural loop known as the anterior forebrain pathway (AFP), Kimpo, Theunissen, and Doupe [26] reported a remarkable precision of the time difference between these pathways of 50 ± 10 ms across many songbirds and many trials.

As we developed models of this phenomenon and its implications, along with excitatory synaptic plasticity at the HVC \rightarrow RA junction, we [27] constructed a circuit of neurons based on detailed electrophysiological measurements by Perkel and his colleagues [28,29], in each of the three nuclei of the AFP. This circuit demonstrated a tunable time delay adjusted by the strength of inhibition at a synapse from the nucleus area X to the nucleus dorsolateral thalamus (DLM). The precise value of the time delay in the birdsong circuit was attributed to a fixed point in the overall dynamics including excitatory synaptic plasticity at the HVC \rightarrow RA junction. This investigation suggested a general form of the time-delay circuit that could be tuned by changing the strength of an inhibitory synaptic connection. A short summary of this idea was presented in [13].

Here we begin with the description of a general neural architecture for the IRU. An essential circuit component in the IRU is a “spike selection unit” (SSU), the purpose of which is to selectively distribute input spikes to downstream elements in the IRU. We present a particular implementation of the SSU circuitry using biologically realistic neuron models. We then present two general schemes for the construction of the time-delay circuitry in the IRU, comprised of excitatory or inhibitory synapses. We discuss general features of the time-delay circuit made up of either excitatory or inhibitory synapses. We then proceed to develop two neural circuits for the full ISI reading unit made up of the SSU, the time-delay circuitry comprised of either excitatory synapses or the inhibitory synapses [13] and the detection unit, which is the output of the IRU.

Next we address the issue of training the IRU using synaptic plasticity rules. We specifically discuss STDP of excitatory synapses (eSTDP) [15,16] in the context of training the IRU consisting of the time-delay circuitry made up of

excitatory synapses and STDP of inhibitory synapses (iSTDP) [14] in the context of the IRU consisting of the time-delay circuitry made up of inhibitory synapses. We show how the IRU can be trained through STDP and how it can be subsequently used to recognize a specific ISI sequence on which it has been trained. Recognition is implemented here through a detection unit that fires an action potential when two input spikes arrive within a short temporal window and responds with a subthreshold activity otherwise. The interaural time difference circuit noted above also uses this kind of coincidence detection to relay information to other neural processes on detection of an appropriate time delay.

The overall IRU circuit comprising a time-delay unit, a spike selection unit, and a detection unit, thus operates by producing a replica of the given ISI sequence. It then uses synaptic plasticity to adjust the delay produced by the time-delay subcircuit to match the ISI in the input sequences to within a chosen resolution threshold of a few msec. Success in this matching is seen in the spiking activity of the detection circuit. The IRU circuit is thus a candidate for how biological networks can accurately select particular environmental signals, potentially usable for further processing for decision making and required functionality, by keying on the representation of environmental signals as a specific spike sequence.

We have also explored the generality of the scheme of spike pattern recognition by an IRU by modeling the IRU circuitry with a simplified phenomenological neuron model using quadratic integrate and fire neurons, retaining the same structure for synaptic currents. While, of course, the results are different in detail, the overall results are essentially the same as when we use HH neuron models. In a sense this is not surprising as the HH models were chosen not to emulate any particular biological neurons but to indicate that conductance based spiking neurons could comprise time-delay units of the form seen in the birdsong circuitry. In this paper we only report results from the IRU constructed with HH type neuron models.

The paper is organized as follows: In Sec. II we begin with the description of the mathematical model for the neurons and the synapses that make up various circuit elements of the IRU. We then present the empirical STDP rules for excitatory and inhibitory synapses used in this work to tune the IRU such that it can selectively respond to the input ISI sequence. In Sec. III, we begin with the description of a general architecture of the IRU circuitry for spike pattern recognition. We then describe neural circuitry for all the essential components of the IRU, beginning with a particular implementation of the spike selection unit. We then describe the circuitry for time delay using excitatory and inhibitory synapses. We then develop the entire IRU circuitry and show how it can be trained to recognize an input ISI sequence using STDP.

II. METHODS

The IRU circuitry described in this work is comprised of two neuron models, namely, (1) a type I neuron and (2) a

bistable neuron. Each neuron model is described in the Hodgkin Huxley framework of a single compartment model and each exhibits a distinct dynamical property in terms of bifurcation from resting state to spiking state as a function of the input current. We also consider three types of synapses in the development of the IRU circuitry. They are (1) excitatory AMPA synapses, (2) excitatory NMDA synapses, and (3) inhibitory GABA_A synapses. The mathematical models for the two neurons and the three synapses are presented below.

A. Neuron models

1. Type I neuron model

We model a type I neuron [30] based on the Hodgkin Huxley framework as a single compartment model with a fast sodium channel, a delayed rectifier potassium channel, and a leak channel. The transition from the resting state to the spiking state in this neuron model occurs through a saddle node bifurcation on the invariant circle [31,32]. The frequency of spiking as a function of input dc current I_{dc} can be given in the form

$$f = C\sqrt{I_{dc} - I_0}, \quad (1)$$

where I_0 is threshold for spiking and the constant C is a function of the model parameters. The dynamical equation for the membrane potential for this model neuron is given by

$$C \frac{dV(t)}{dt} = I_{dc} + g_{Na}m^3(t)h(t)(E_{Na} - V(t)) + g_Kn^4(t)(E_K - V(t)) + g_L(E_L - V(t)) + I_S(t). \quad (2)$$

$C=1 \mu\text{F}/\text{cm}^2$. $V(t)$ is the membrane potential, I_{dc} : external dc current drive, is set such that the neuron spikes at an intrinsic frequency f , given in Eq. (1). $I_S(t)$ is the synaptic current. E_r ($r=\text{Na}, \text{K}, \text{L}$) are reversal potentials of the sodium and potassium ion channels and the leak channel, respectively. g_r ($r=\text{Na}, \text{K}, \text{L}$) represent the conductance of sodium, potassium, and the leak channel, respectively. All the parameters for the neuron model are summarized in Table I.

The gating variables $X=\{m, h, n\}$ satisfy the first order kinetic equation: $\frac{dX(t)}{dt} = \alpha_X(V(t))(1-X(t)) - \beta_X(V(t))X(t)$, where α_X and β_X are given below with $V_{th}=-65$ mV.

$$\alpha_m = \frac{0.32(13 - (V(t) - V_{th}))}{e^{(13-(V(t)-V_{th}))/4.0} - 1}, \quad \beta_m = \frac{0.28((V(t) - V_{th}) - 40)}{e^{((V(t)-V_{th})-40)/5} - 1},$$

$$\alpha_h = 0.128e^{17-(V(t)-V_{th})/18}, \quad \beta_h = \frac{4}{e^{40-(V(t)-V_{th})/5} + 1},$$

$$\alpha_n = \frac{0.032(15 - (V(t) - V_{th}))}{e^{(15-(V(t)-V_{th})/5} - 1}, \quad \beta_n = \frac{0.5}{e^{(V(t)-V_{th})-10/40}}.$$

2. Bistable neuron model

We model the bistable neuron in the Hodgkin Huxley framework as a single compartment model with a persistent sodium channel, a fast potassium channel, and the leak current. The transition from the resting state to the spiking state

TABLE I. Model parameters used in all calculations, unless otherwise mentioned in the figure caption.

Type I neuron model	E_{Na}	50 mV
	E_K	-95 mV
	E_L	-64 mV
	g_{Na}	215 mS/cm ²
	g_K	43 mS/cm ²
	g_L	0.813 mS/cm ²
Bistable neuron model	E_{Na}	60 mV
	E_K	-90 mV
	E_L	-80 mV
	g_{Na}	20 mS/cm ²
	g_K	10 mS/cm ²
	g_L	8 mS/cm ²
	V_m	-20 mV
	V_n	-25 mV
	k_m	15 mV
	k_n	5 mV
	τ_n	0.16 mV

in this model occurs through a saddle node off-invariant circle, bifurcation [32]. As a result there is a coexistence of a stable resting state (fixed point) and a stable spiking state (limit cycle) just before the bifurcation and either an excitatory and inhibitory input pulse can result in transition of the dynamics between the stable resting and the stable spiking states [32]. The dynamical equation for the membrane potential for this model neuron is given by

$$C \frac{dV_B(t)}{dt} = g_{Na}m_\infty(V(t))(E_{Na} - V_B(t)) + g_Kn(t)(E_K - V_B(t)) + g_L(E_L - V_B(t)) + I_S(t) + I_{dc1}, \quad (3)$$

$C=1 \mu\text{F}/\text{cm}^2$. $V_B(t)$ is the membrane potential of the bistable neuron, I_{dc1} , external dc current drive. $I_S(t)$ is the synaptic current. E_r ($r=\text{Na}, \text{K}, \text{L}$) are reversal potentials of the sodium and potassium ion channels and the leak channel, respectively. g_r ($r=\text{Na}, \text{K}, \text{L}$) represent the conductance of sodium, potassium, and the leak channel, respectively. Again all the parameters for the neuron model are summarized in Table I.

The gating variable $n(t)$ satisfies the following first order kinetic equation:

$$\frac{dn(t)}{dt} = \frac{n_\infty(V(t)) - n(t)}{\tau_n}.$$

The activation functions $X_\infty(V)=\{m_\infty(V), n_\infty(V)\}$ depend on voltage V as

$$X_\infty(V) = 1/(1 + \exp((V_X - V)/k_X)),$$

where V_X and k_X are the parameters of the activation function, given in Table I.

B. Synapse model

The synaptic currents are given as

(1) Excitatory AMPA synapse: $I_S(t) = g_a S^E(t)(E_E - V(t))$, where g_a is the synaptic conductance, $E_E = 0$ mV is the reversal potential for an excitatory synapse, and $S^E(t)$ is the gating variable, which determines the fraction of bound glutamate neurotransmitters relative to the maximum neurotransmitters that can be bound, $0 \leq S^E(t) \leq 1$.

(2) Excitatory NMDA synapse: $I_S(t) = g_n B(V(t)) S^E(t)(E_E - V(t))$, where g_n is the synaptic conductance and $B(V) = 1.0 / (1 + 0.288 \exp(-0.062V))$. E_E and $S^E(t)$ represent the same quantities as described above, however, time constants for the AMPA $S^E(t)$ and the NMDA $S^E(t)$ are quite different as described below.

(3) Inhibitory GABA_A synapse: $I_S(t) = g_g S^I(t)(E_I - V(t))$, where g_g is the synaptic conductance, $E_I = -75$ mV is the reversal potential of inhibitory synapse, and $S^I(t)$ is the gating variable, which determines the fraction of bound GABA_A neurotransmitters relative to the maximum neurotransmitters that can be bound, $0 \leq S^I(t) \leq 1$.

The $S^Y(t)$ ($Y = \{E, I\}$) satisfy the following first order kinetic equation:

$$\frac{dS^Y(t)}{dt} = \frac{S_0(\theta(t)) - S^Y(t)}{\hat{\tau}(S_1 - S_0(\theta(t)))},$$

where $\theta(t) = \sum_i \Theta(t - t_i) \Theta((t_i + \tau_R) - t)$. $\Theta(X)$ is the Heaviside function satisfying $\Theta(X) = 1$ if $X > 0$ else $\Theta(X) = 0$ and t_i is the time of the i th presynaptic neuronal spike. The kinetic equation for $S^Y(t)$ involves two time constants: $\tau_R = \hat{\tau}(S_1 - 1)$, the docking time for the neurotransmitter and $\tau_D = \hat{\tau}S_1$, the undocking time constant for the neurotransmitter binding. The characteristic time scales for an AMPA synapse are chosen such that $\tau_R = 0.1$ ms and $\tau_D = 1.5$ ms. For the slow NMDA synapse the time scales are $\tau_R = 2.5$ ms and $\tau_D = 70$ ms. For the inhibitory GABA_A synapse the time scales are $\tau_R = 1.1$ ms and $\tau_D = 5.5$ ms. Finally, $S_0(\theta)$ is the sigmoidal function given by $S_0(\theta) = 0.5(1 + \tanh(120(\theta - 0.1)))$.

C. STDP

1. eSTDP

We consider a generic form of eSTDP [15,16,33,34]. The synaptic modification arising from a single pair of pre- or postsynaptic spikes is given through function $\Delta g(\Delta t)$, given by [35]

$$\begin{aligned} \Delta g(\Delta t) &= \frac{\gamma \alpha_p \alpha_D^\eta}{\beta_p + \eta \beta_D} e^{-\beta_p \Delta t} - \frac{\gamma \alpha_D \alpha_p^\eta}{\eta \beta_p + \beta_D} e^{-\eta \beta_p \Delta t} & \text{if } \Delta t \geq 0 \\ &= \frac{\gamma \alpha_p \alpha_D^\eta}{\beta_p + \eta \beta_D} e^{\eta \beta_D \Delta t} - \frac{\gamma \alpha_D \alpha_p^\eta}{\eta \beta_p + \beta_D} e^{\beta_D \Delta t} & \text{if } \Delta t < 0, \end{aligned} \quad (4)$$

where $\Delta t = t_{\text{post}} - t_{\text{pre}}$ is the time difference between a postsynaptic spike at t_{post} and a presynaptic spike at time t_{pre} . In Fig. 1(a) we show the eSTDP rule fit with a function given in Eq. (4) for parameters [35], $\gamma = 10^{-9}$, $\alpha_p = \alpha_D = 33.5$, $\beta_p = 0.098$ ms⁻¹, $\beta_D = 0.035$ ms⁻¹, and $\eta = 4$.

2. iSTDP

A spike timing dependent plasticity rule for inhibitory synapses (iSTDP) has been recently reported in [14] and an

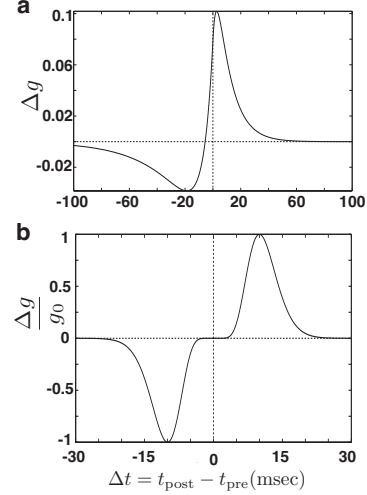


FIG. 1. STDP rules. (a) STDP of excitatory synapse. The parameter values for the learning rule described through Eq. (4) are $\gamma = 10^{-9}$, $\alpha_p = \alpha_D = 33.5$, $\beta_p = 0.098$ ms⁻¹, $\beta_D = 0.035$ ms⁻¹, and $\eta = 4$. (b) STDP of inhibitory synapse. The parameter values for the learning rule as described through Eq. (5) are $\alpha = 1$ and $\beta = 10$.

empirical fit to the observed experimental data was obtained with the following functional form:

$$\Delta g(\Delta t) = \frac{g_0}{g_{\text{norm}}} \alpha^\beta |\Delta t| \Delta t^{\beta-1} e^{-\alpha |\Delta t|}, \quad (5)$$

where $\Delta t = t_{\text{post}} - t_{\text{pre}}$. g_0 is a scaling factor accounting for the amount of change in inhibitory conductance induced by the synaptic plasticity rule. $g_{\text{norm}} = \beta e^{-\beta}$ is a normalizing constant. With parameter values $\alpha = 1$ and $\beta = 10$, we obtain a window of ± 20 ms over which the efficacy of synaptic plasticity is nonzero. In Fig. 1(b), we show the iSTDP rule fit with a function given in Eq. (5). We plot $\Delta g(\Delta t)/g_0$ as a function of Δt for the parameter values $\alpha = 1$ and $\beta = 10$.

III. RESULTS

Given an input sequence of spikes at times $\{t_0, t_1, t_2, \dots, t_n\}$, encoding a stimulus signal in the ISIs: $T_i = t_{i+1} - t_i$ ($i = 1, 2, \dots, n-1$), we describe a general framework for a neuronal circuit comprised of a network of neurons interacting through synaptic connections that is capable of decoding the information about the stimulus embedded in the sequence of ISIs. We define “decoding” as the ability of the neural circuit to respond to the incoming ISI sequence that encodes the information about the stimulus and produces no response to any other input ISI sequence. In Fig. 2 we show the schematic diagram of such neural circuitry and we refer to it as IRU.

In order to understand the principle behind the IRU ability to recognize a given ISI sequence that encodes the stimulus information, we consider an input spike sequence comprised of two spikes at times $\{t_0, t_0 + T\}$. The input arrives to the IRU at the SSU, whose function it is to selectively distribute input spikes to downstream components in the IRU. Specifically, as we see from Fig. 2 the SSU feeds the input spike at time t_0 , to the “time-delay unit” (TDU) and the spike at time

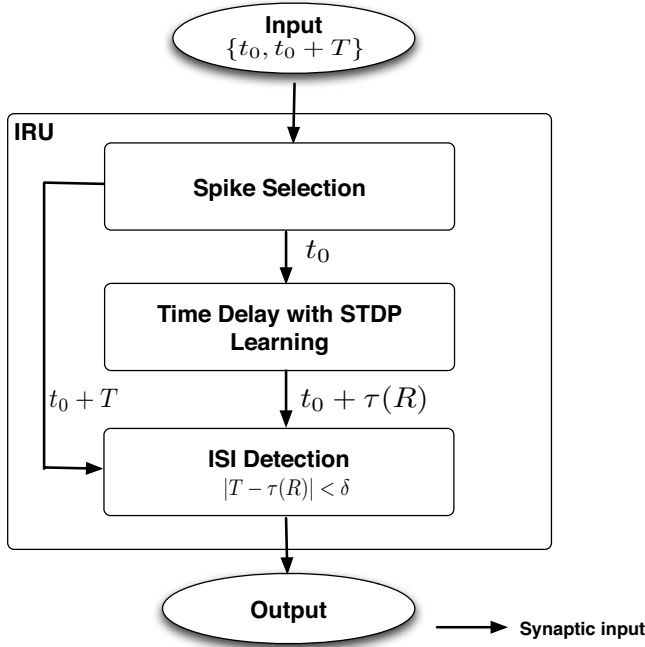


FIG. 2. Schematic diagram of the IRU neural circuitry. It consists of three essential components, namely, (1) the SSU, (2) the tunable TDU, which can be tuned through the tunable parameter R that can be modulated by STDP, and (3) a DU. Input to the IRU is a spike sequence $S=\{t_0, t_0+T\}$ and the output from the IRU, for the correct tuning parameter R is a single spike corresponding to the recognition of the input ISI, T , implying that the IRU has decoded the information contained in the ISI of length T ms.

t_0+T to the “detection unit” (DU). The TDU reads the input spike and emits an output spike at time $t_0+\tau(R)$, where R is the tunable parameter of the TDU. The two spikes at times t_0+T and $t_0+\tau(R)$ arrive at the DU, which acts as a coincidence detector and responds to the incoming spikes depending on the time difference $|T-\tau(R)|$. If $|T-\tau(R)|>\delta$, where δ is the resolution of spike pair detection by the DU, STDP modulates the synaptic strength of the synapses in the IRU, specifically the tuning parameter R within the TDU, so that $|T-\tau(R)|\rightarrow\delta$. The IRU is considered trained when $|T-\tau(R)|\leq\delta$ such that the DU responds with an output spike and the tuned parameter R of the IRU has evolved to a final steady state value. Subsequent presentation of the spike sequence will then successfully elicit an output spike from the IRU implying its ability to “decode” the information embedded in the input ISI sequence. This process is a nonlinear dynamical system of the form of an iterated map: $R_n\rightarrow R_{n+1}=f(R_n)$, where $f(R)$ is the action of the IRU on the presentation of $n=1, 2, \dots$ ISIs. We seek a stable fixed point of this map interpreted in terms of the ability of the IRU to “decode” the information in the input ISI sequence.

We now describe in detail each circuit within the IRU, made up of biologically realistic neuron models and synaptic connections, and explain how the IRU can utilize STDP to train itself to respond to the correct temporal sequence of input spikes.

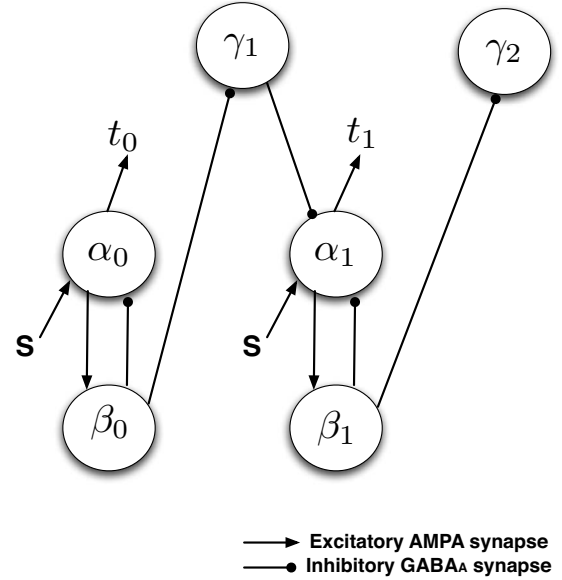


FIG. 3. SSU. The SSU performs the task of selectively distributing the spikes in the input interspike interval sequence to the downstream IRU components. Input to the SSU is the spike sequence $S=\{t_0, t_1, \dots\}$ and the output is a single spike from neural units α_i at times t_i corresponding to spike times in the sequence S . In the example shown the input to the SSU is S , which represents a pair of spikes at times $\{t_0, t_1\}$ and the output is a single spike from a neural unit α_0 at time t_0 and another spike output from neural unit α_1 at time t_1 . The conductance of the excitatory AMPA synapses $g_{\alpha\beta}=1$ mS/cm², the inhibitory GABA_A synapses $g_{\beta\alpha}=70$ mS/cm², and $g_{\beta\gamma}=7$ mS/cm².

A. SSU and the DU

In Fig. 3 we show the schematic of the spike selection unit (SSU). The primary purpose of this circuitry is to split incoming spikes and distribute them appropriately to the downstream components of the IRU circuitry to be used in the IRU training and later for the task of spike pattern recognition. Neural units β_n and γ_n of the SSU are bistable neurons (Sec. II A 2). Absent any input to the SSU, neurons γ_n are in the stable spiking state and neurons β_n are in the stable resting state. Neurons α_n of the SSU are type I HH neurons (Sec. II A 1) and are at a stable resting state. The conductance of the excitatory AMPA synapse from neurons $\alpha\rightarrow\beta$ in the SSU are $g_{\alpha\beta}=1$ mS/cm² (g_{ij} represents the synapse from neuron i to neuron j). The conductance of inhibitory GABA-A synapses from neurons $\beta\rightarrow\alpha$ and $\beta\rightarrow\gamma$ are $g_{\beta\alpha}=70$ mS/cm² and $g_{\beta\gamma}=7$ mS/cm², respectively.

In general SSU can select spikes from a sequence of spikes at times $\{t_0, t_1, \dots, t_N\}$. Here we concentrate on $N=2$ to illustrate the operation of the SSU without any loss of generality. For the case $N=2$ input to the SSU is the spike sequence $S=\{t_0, t_1=t_0+T\}$, where T is the interspike interval. When the first input spike at time t_0 arrives at neuron α_0 , it responds and the SSU emits an output spike at time t_0 . The activity of neuron α_0 excites neuron β_0 and the excitatory drive through an AMPA synapse from neuron α_0 to neuron β_0 pushes the neuron into its bistable spiking state. The spiking neuron β_0 now inhibits neuron α_0 through an inhibitory

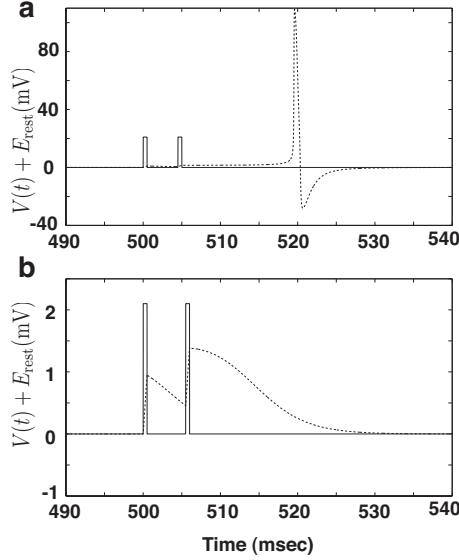


FIG. 4. Response of the DU to two incoming spikes. (a) The DU responds with an output spike when it receives two input spikes within $\delta \leq 4$ ms. The output spike occurs about 15 ms later, corresponding to the integration time scale of the neuronal dynamics. The two incoming spikes are represented as rectangular pulses shown in the figure, scaled appropriately for visualization. (b) The DU responds with a subthreshold excitatory postsynaptic potential, in response to two input spikes arriving at the DU with a delay $\delta > 4$ ms. The model parameters are $I_{dc} = 0.99$ mA/cm² and $g_{in} = 0.05$ mS/cm².

GABA-A synapse and α_0 no longer responds to any further input spikes. β_0 also inhibits neuron γ_1 moving it from its bistable spiking state to the stable resting state. Until this point in time, neuron γ_1 is inhibiting neuron α_1 . The quieting of γ_1 allows α_1 to respond to spikes in S at t_1 producing an output spike at time t_1 . Neuron β_1 is now excited into a stable oscillating state and it inhibits α_1 and γ_2 . α_1 no longer responds to any further spikes in the sequence S . Not shown in Fig. 3 is the final step in the SSU implementation whereby all neurons β_n are returned to rest and all neurons γ_n are returned to their stable oscillating state, which represents the initial dynamical configuration of the SSU. This can be accomplished by a global inhibition of β_n and excitation of γ_n after S has stimulated output spikes from all neurons α_n .

The detection unit (DU) is implemented in the IRU in the form of a single type I HH neuron which acts as an integrator and responds with an output spike in response to two input spikes, through an AMPA excitatory synapse (synaptic conductance g_{in}) arriving within δ msec. For the parameters of the DU circuitry ($I_{dc} = 0.99$ mA/cm², $g_{in} = 0.05$ mS/cm²) considered in Fig. 4, $\delta = 4$ ms. In Fig. 4(b), we show the response of the DU when it receives two input spikes 5 ms apart. The total integrated current entering the DU at the given interval of 5 ms between the two incoming spikes is not sufficient to push the neuron beyond its spiking threshold and the neuron responds with a subthreshold excitatory postsynaptic potential. As shown in Fig. 4(a) when the input spikes are sufficiently close in time ≤ 4 ms, the total integrated input is sufficient to push the neuron above its spiking threshold. It now responds with an output spike after a delay

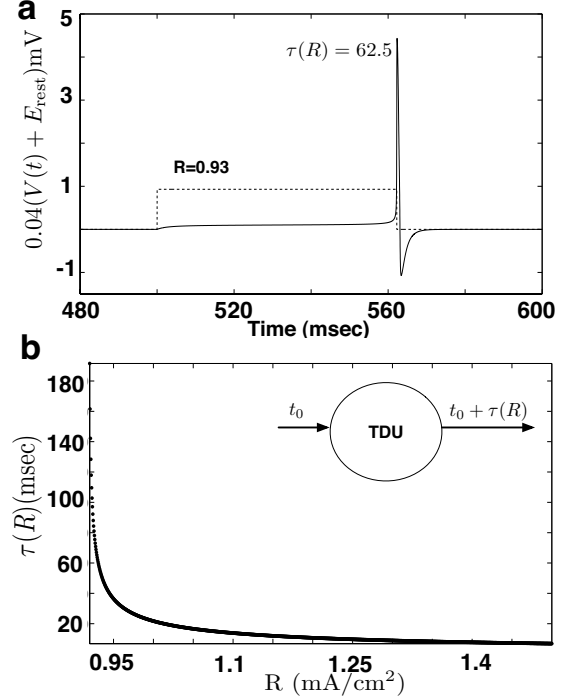


FIG. 5. One neuron TDU. In the inset of (b) we show the schematic diagram of a single neuron TDU, made up of a type I HH neuron. It receives input current $I_S(t) = R[\theta(t - t_0) - \theta(V(t) - V_{th})]$ starting at time t_0 . Depending on the strength of input current parameter R , the neuron responds with a spike output at time $t_1 = t_0 + \tau(R)$. (a) We show (solid line) the membrane potential of the single neuron TDU when $R = 0.93$. In this case the neuron responds with a delay of $\tau(R) = 62.5$ ms. The dotted line represents the input current $I_S(t)$ to the neuron. (b) We plot the variation in the delay $\tau(R)$ produced by the neuron as a function of the parameter R . The model parameters are $I_{dc} = 1.0$ mA/cm².

of about 15 ms. The DU thus acts as a coincidence detector producing a response spike if it receives two simultaneous spike inputs (within $\delta = 4$ msec).

B. TDU

We present two distinct architectures for the TDU circuitry comprised of tunable excitatory and inhibitory synapses, respectively. The essential function of the TDU is to read an input spike at time t_0 and respond with an output spike after a time $t_0 + \tau(R)$, where R is the tunable parameter of the TDU which can be modulated through STDP.

1. Concept of a TDU

We begin with the description of the simplest time-delay circuitry comprised of a single type I HH neuron. This is shown schematically in the inset of Fig. 5(b). The input to the neuron is the current $I_S(t) = R[\Theta(t - t_0) - \Theta(V(t) - V_{th})]$, where $\Theta(x) = 0$ when $x \leq 0$ and $\Theta(x) = 1$ when $x > 0$. t_0 is the time of the input spike to the neuron. The parameter I_{dc} [Eq. (2)] is set at 1.0 mS/cm², resulting in the resting potential of the neuron $E_{rest} \approx -62$ mV. V_{th} is the threshold for detecting action potential and is set to 0 mV. The spike output from

the neuron occurs at time t_1 when the membrane voltage exceeds V_{th} . The time delay of the output spike is then, $\tau(R) = t_1 - t_0$. The input current $I_S(t)$ turns on a constant current R at time t_0 and the membrane voltage of the neuron integrated through the HH dynamics [Eq. (2)], increases until the voltage rises above V_{th} and a spike appears at time t_1 . At t_1 the current $I_S(t)$ is turned off.

Using this type I neuron model, with step input current until a spike output is generated from the TDU, we can construct a TDU to obtain various time delays as a function of the strength of R . In Fig. 5(a) we show a sample trace of the output from the single neuron delay unit for $R \approx 0.93$ leading to $\tau(R) \approx 62.5$ msec.

In Fig. 5(b) we show the delay $\tau(R)$ as a function of R from this one neuron model. We note that for $R=0$, the TDU will not receive any input current and will therefore never produce an output spike, resulting in $\tau(R=0) \rightarrow \infty$. For very large R we expect $\tau(R) \rightarrow 0$, since the neuron receives a very high input current to drive it to spiking threshold rapidly. The one neuron model does not involve any synapses, so synaptic plasticity cannot be used to train the time delay to a desired value. Further, though the neuron is a biologically realistic HH model neuron, the circuit requires a step current input which is not.

2. TDU with excitatory synapses

Building on the idea underlying the construction of a single neuron TDU, we construct a two neuron model of the TDU that is biologically feasible. The inset of Fig. 6(b) shows the schematic diagram of the two neuron TDU. Neuron β is a bistable neuron, in resting state. It synapses onto neuron α , a type I neuron, through an excitatory NMDA synapse. α in turn synapses onto β through an inhibitory GABA-A synapse. The input spike arrives into neuron β at time t_0 through an excitatory AMPA synapse and at the same time into neuron α through a tunable excitatory NMDA synapse with synaptic strength $g_S = Rg_{S0}$ ($g_{S0} = 1$ mS/cm²). The output of the TDU is from neuron α at time t_1 at time delay of $\tau(R) = t_1 - t_0$. The time delay $\tau(R)$ can be modulated by changing the synaptic strength g_S , through the tunable parameter R . A single input spike at time t_0 drives β into its stable spiking state providing enough depolarizing current to neuron α until it fires at time t_1 . In order for the spiking neuron β to provide enough depolarization for neuron α to eventually fire, the firing frequency of neuron β should be greater than the inverse decay time of the excitatory synaptic connection from β to α . This is achieved by using a slow NMDA type excitatory synaptic connection from β to α . A spike from neuron α at time $t_1 = t_0 + \tau(R)$ then provides a hyperpolarizing input to neuron β and sets it back into its rest state. Depending on the synaptic strength g_S , neuron α is pushed closer to spiking threshold sooner thereby allowing the modulation of the time delay produced by the TDU.

In Fig. 6(a) we show a sample trace of the output from the TDU through neuron α (in black), the input to the TDU at time t_0 (a scaled input pulse, shown by a black dotted line), and the activity of the bistable neuron β (shown in red) as a function of time. In this particular example the delay observed is around 134.5 msec. In Fig. 6(b) we show a plot of

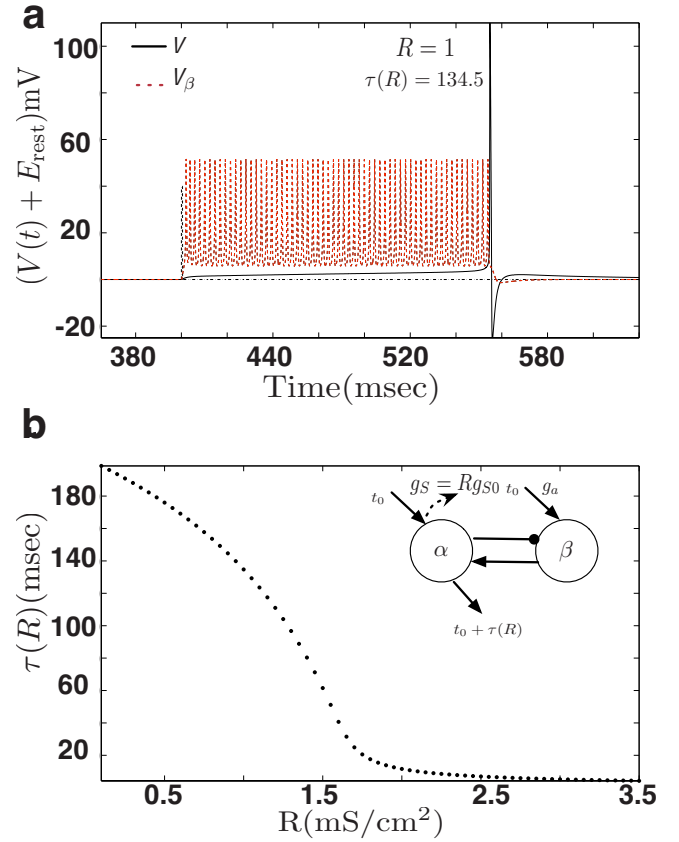


FIG. 6. (Color online) TDU with an excitatory synapse. In the inset of (b) we show the schematic diagram of the TDU with excitatory synapse. It receives input at time t_0 through an excitatory synapse with strength $g_S = Rg_{S0}$. Depending on the excitatory synaptic strength R , the TDU responds with a spike output at time $t_1 = t_0 + \tau(R)$. (a) We show the membrane potential of the two neurons in the TDU, neuron α (solid-black line) and neuron β (dotted red-line) and a rectangular pulse (scaled for visualization) corresponding to input received by the TDU at time t_0 when $R=1.0$. In this case the neuron responds with a delay of $\tau(R) = 134.5$ ms. (b) We plot the variation in the delay $\tau(R)$ produced by the TDU as a function of the parameter R . The strength of excitatory NMDA synapse $g_{\beta\alpha} = 3.5$ mS/cm², the excitatory AMPA synapse onto the bistable neuron $g_a = 0.1$ mS/cm², and the inhibitory GABA_A synapse $g_{\alpha\beta} = 0.5$ mS/cm². The dc currents, $I_{dc} = 0.5$ mA/cm² and $I_{dc1} = 4.0$ mA/cm².

the time delay of this model $\tau(R)$. This dependence of $\tau(R)$ on a synaptic strength $g_S = Rg_{S0}$, through the tunable parameter R is typical for excitatory synapses. As the excitation increases, the time to produce a delayed spike output decreases. This monotonic decreasing ($\frac{d\tau(R)}{dR} < 0$) relation of the time delay produced by the TDU with excitatory synapses in conjunction with eSTDP [Eq. (4)] results in a stable learning mechanism by which the IRU can train itself to recognize a temporal sequence of the input spike train, as will be shown in Sec. III C.

3. TDU with inhibitory synapses

The TDU with inhibitory synapses is motivated by and abstracted from the AFP in the songbird brain. This particu-

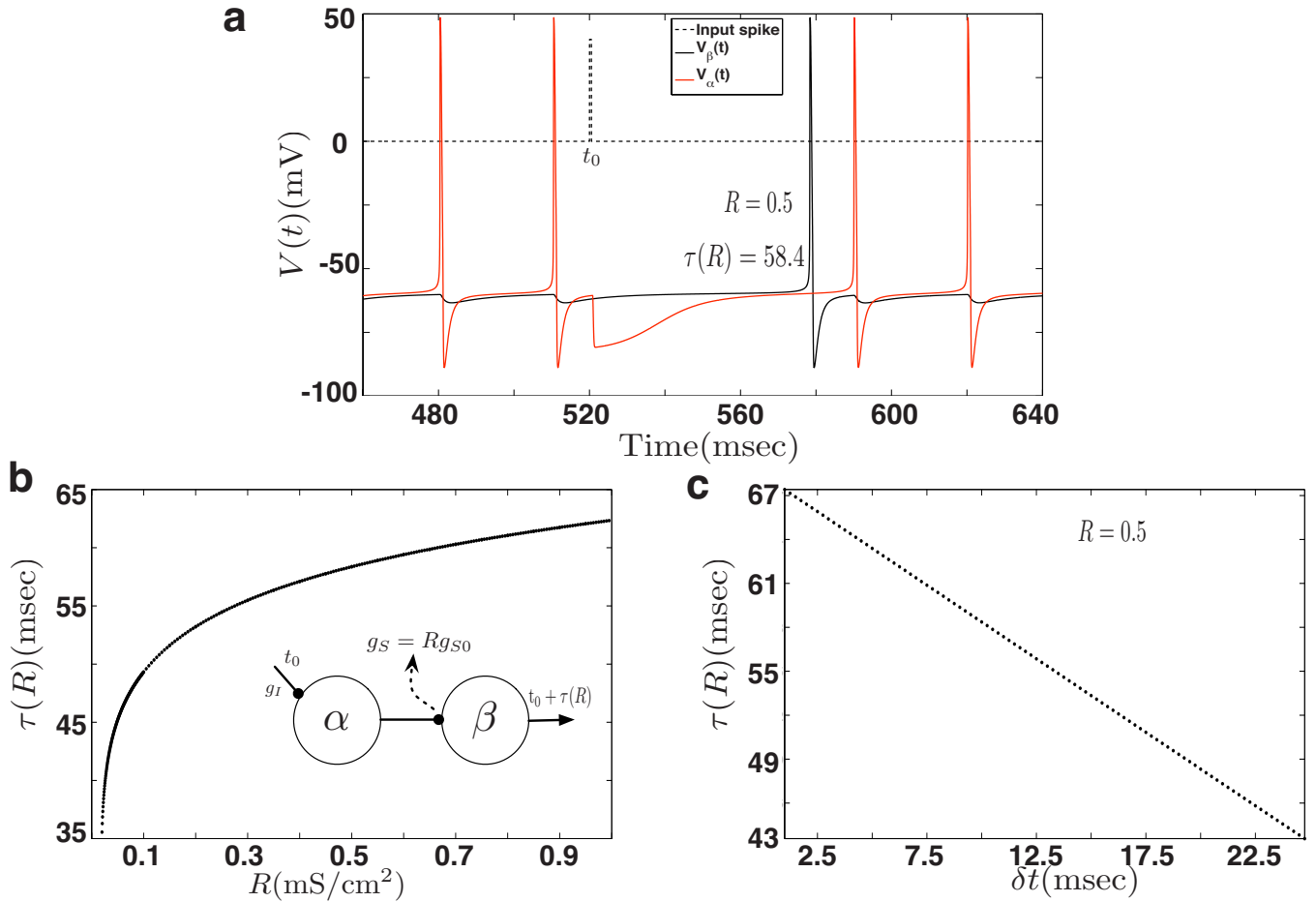


FIG. 7. (Color online) Two neuron time-delay unit with an inhibitory synapse. In the inset of (b) we show the schematic diagram of the TDU with inhibitory synapse. It receives input at time t_0 through an inhibitory synapse. Depending on the excitatory synaptic strength R of the synapse from $\alpha \rightarrow \beta$, the TDU responds with a spike output at time $t_1 = t_0 + \tau(R)$. (a) We show the membrane potential of the two neurons in the TDU, neuron α (red) and neuron β (black) and an input rectangular pulse (scaled for visualization) corresponding to input received by the TDU at time t_0 when $R = 0.5$. In this case the neuron responds with a delay of $\tau(R) = 134.5$ ms. (b) We plot the variation in the delay $\tau(R)$ produced by the TDU as a function of the parameter R . (c) We plot the variation of $\tau(R)$ as a function of δt , the relative time of the input spike arriving into α with respect to the oscillation period of spiking for α , when $R = 0.5$. The dc currents $I_{dc}^\alpha = 1.94$ mS/cm², $I_{dc}^\beta = 1.93$ mS/cm². The strength of inhibitory GABA_A synapse $g_I = 50$ mS/cm².

lar architecture of the TDU and its utility in spike pattern recognition was summarized in [13]. In this section we explore in detail the abstraction of the TDU with inhibitory synapses from the songbird AFP.

We begin by constructing a simple two neuron time-delay circuit with inhibitory synapse as shown in Fig. 7(b) (inset). This two neuron time-delay circuit is composed of an oscillating neuron α , which projects synaptic inhibition to another neuron β , which under the influence of this inhibition remains below spiking threshold. In the absence of spike input to neuron α , neuron β never produces a spike output. When a spike arrives at α at time t_0 through an inhibitory input synapse, α 's oscillation is turned off releasing inhibition on neuron β and it responds with a spike output at time $t_0 + \tau(R)$. Neuron β can respond with varying time delay $\tau(R)$, dependent on the strength of inhibition $g_S = Rg_{S0}$ ($g_{S0} = 1$ mS/cm²) from $\alpha \rightarrow \beta$. Both neuron α and neuron β are represented by a type I HH neuron model [Eq. (2)]. The strength of the dc current in neuron α , $I_{dc}^\alpha = 1.94$ mS/cm². In

the absence of any other synaptic input, neuron α oscillates with an intrinsic period $T \approx 30$ msec.

In Fig. 7(a), we show a sample trace for the membrane voltage of neurons, α and β in response to a spike received by α at time $t_0 = 520$ ms (shown by a dotted black line) when $R = 0.5$. In this case neuron β responds with a spike output at time $t_0 + \tau(R)$ with $\tau(R) = 58.4$ msec. In Fig. 7(b), we plot $\tau(R)$ as a function of the tunable parameter R , when the input spike arrives at neuron α at time $t_0 = 520$ msec.

For this configuration of the time-delay circuit, the output spike produced by neuron β at time $t_0 + \tau(R)$ for a given strength of inhibition $g_S = Rg_{S0}$, depends on the relative timing of the input spike arriving at neuron α at time t_0 with respect to the oscillation period of α . If we denote T_L as the time of the last spike from neuron α before the arrival of the input pulse into the TDU at time t_0 , such that $T_L \leq t_0$, then the relative timing of the arrival of the input pulse is given by $\delta t = t_0 - T_L$. The dependence of the delayed output spike from β as a function of δt is shown in Fig. 7(c). We see that the

time of the output spike from the time-delay unit in this configuration not only depends on the strength of tunable parameter R [Fig. 7(b)], but also depends on the timing of the arrival of the input spike into neuron α at time t_0 relative to the period of oscillation of α [Fig. 7(c)]. Thus for given R , the timing of the delayed spike output from the TDU varies over the period of oscillation of neuron α , which is not a desirable outcome for the TDU in its utility for the construction of the IRU circuitry.

4. Three neuron TDU with inhibitory synapses

We modify the simple two neuron time-delay circuit described above to a three neuron model with a tunable inhibitory synapse, such that the output of the circuit is dependent only on the strength of synaptic inhibition and is independent of the relative timing of the arrival of the input pulse. The modified three neuron time-delay circuit, shown in Fig. 8(b), is abstracted from the observed anatomical structure of the AFP in the brain of songbirds as shown in Fig. 8 [28,29].

The AFP of songbirds is comprised of three nuclei: area X, DLM, and lateral part of the magnocellular nucleus of the anterior neostriatum (LMAN), as shown in Fig. 8(a), each having a few times 10 000 neurons [36,37]. The input to the AFP is via a sparse burst of spikes from nucleus HVC entering area X. The output signal of the AFP is from LMAN leaving the AFP to innervate the RA nucleus. Within area X two distinct neuron types, spiny neurons (SN) and aspiny fast firing (AF) neurons, receive direct innervation from HVC [28,38]. In the absence of signals from HVC the SNs are at rest while the AF neurons are oscillating at about 20–25 Hz. The SNs inhibit the AF neurons, and these in turn inhibit neurons in DLM, a thalamic nucleus in the AFP [39]. The DLM neurons receiving this input from area X are driven by the inhibition received from AF below the threshold for action potential production and do not produce action potentials while the AF neuron oscillates. When the AF \rightarrow DLM inhibition is released, the DLM neurons rebound and fire periodic action potentials. These propagate to LMAN and are then transmitted to RA. The time around this path is observed to differ from the direct HVC \rightarrow RA innervation by 50 ± 10 ms [26,27].

In our model for the AFP circuitry [27], treating each nucleus as a coherent action potential generating device, we found that LMAN played an unessential role in determining the time delay around the AFP while the strength of the AF \rightarrow DLM inhibition could tune the time delay over a range of 10–100 ms.

From these observations and motivated by the simple two neuron construction of the time-delay circuit we have constructed a biologically feasible time-delay circuit comprised of three neural units and two inhibitory synapses with a tunable synaptic strength. The time-delay circuit is displayed in Fig. 8(b). Neuron α (similar to the SN in area X) receives an excitatory input signal from some source. It is at rest when the source is quiet and when activated, it inhibits neuron β (similar to the AF neuron in area X). Neuron β receives an excitatory input from the same source and it oscillates periodically when there is no input from the source. Neuron β inhibits neuron γ (similar to a DLM neuron). Neuron γ pro-

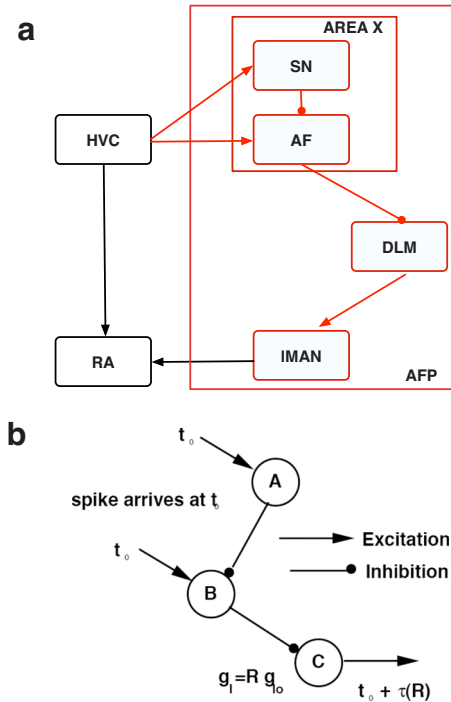


FIG. 8. (Color online) Schematic diagram of the three neuron time-delay unit used in the IRU circuit. This is abstracted from a time-delay network in the AFP of the birdsong system as shown in red in the schematic diagram at the top of the figure. The diagram shows the AFP loop (area X, DLM, and IMAN) from the birdsong system that suggested our three neuron time-delay unit. Unit A is abstracted from the area X SN neurons, unit B is abstracted from the area X AF neurons, and unit C is abstracted from the thalamic excitatory neurons in DLM. Absent any input spikes, neuron A is at rest, neuron B oscillates periodically, and neuron C oscillates around its rest potential driven by periodic inhibitory input from neuron B. When an input spike arrives at neuron A and at neuron B at time t_0 , neuron A fires an action potential and neuron B has the phase of its oscillation reset to be in synchrony with the time of arrival t_0 of the spike. The action potential in neuron A inhibits neuron B, and this releases neuron C to rise to its spiking threshold a time $\tau(R)$ later. R is the dimensionless scale of the $B \rightarrow C$ inhibition. Within a broad range for R , neuron C will fire a single spike at a time $t_0 + \tau(R)$. The value of the conductance for the $B \rightarrow C$ inhibitory synapse is $g_I = R g_{I0}$, with g_{I0} a baseline conductance.

duces periodic spiking in the absence of inhibition from neuron β . The tunable synapse is the inhibitory synapse from neuron β to neuron α .

Each of the neurons α , β , and γ is represented by a type I HH neuron with sodium, potassium, and leak currents as well as an injected dc current to set the spiking threshold [Eq. (2)]. A more detailed neuron model for neuron γ could include hyperpolarization activated I_h channels and low threshold calcium I_T channels, which facilitate post inhibitory rebound spikes [27]. Indeed, in the DLM neuron of the birdsong AFP this mechanism leads to calcium spikes as the output of neuron γ .

When the inhibition from neuron β to neuron γ is released as a result of an inhibitory signal from neuron α onto neuron β , neuron γ rebounds and produces an action potential some time later. This is due to the intrinsic stable spiking

state of neuron γ in the absence of any inhibition from neuron β . The time delay for neuron γ to produce a spike is dependent on the strength of the $\beta \rightarrow \gamma$ inhibition $g_I = Rg_{I0}$ ($g_{I0} = 1$ mS/cm²). The stronger the inhibition g_I onto neuron γ , its membrane potential driven is further below threshold and as a result, the longer is the duration required for the membrane voltage to reach the threshold for action potential generation. This means the larger the $\beta \rightarrow \gamma$ inhibition, the longer the time delay produced by the circuit. Other parameters in the circuit, such as the membrane time constants, set the scale of the overall time delay that can be produced by the circuitry.

The direct excitation of neuron β by the signal source is critical. It serves to reset the phase of the neuron β oscillation, as a result of which the time of the spike from neuron γ is measured with respect to the input signal and thus makes the timing of the circuit precise relative to the arrival of the initiating spike. Without this excitation to neuron β , the phase of its oscillation is uncorrelated with the arrival time of the signal from the source, and the time delay of the circuit varies over the period of oscillation of neuron β as was the case with two neuron construction of the TDU with inhibitory synapses. This is not a desirable outcome, nor is it the way the AFP circuit appears to work [28].

For the conductance values $g_{\alpha\beta} = 50$ mS/cm², $g_{\beta\gamma} = g_S = Rg_{S0}$, with $g_{S0} = 1$ mS/cm² and $R = 0.05$ and excitatory inputs at neuron α and β , $g_\alpha = g_\beta = 0.5$ mS/cm², and $I_{dc}^\alpha = 1$ mA/cm², resulting in $E_{rest}^\alpha \approx -62$ mV, $I_{dc}^\beta = 1.94$ mS/cm², and $I_{dc}^\gamma = 1.93$ mS/cm² we find the delay produced by the TDU, $\tau(R) \approx 54.5$ msec, as shown in Fig. 9(b). For R too small, $R \leq 0.019$ in Fig. 9(b), the inhibition from $\beta \rightarrow \alpha$ does not prevent production of action potentials through the default spiking state of neuron γ in the absence of inhibition. For R too large, $R \geq 0.77$ in Fig. 9(b), the neuron γ is inhibited so strongly it never spikes. Over the range of $0.019 \leq R \leq 0.77$ we typically find $\tau(R)$ ranges over about 20 ms within an overall scale of about 10–100 ms, depending on the integration time constants in Eq. (2). In Fig. 9(a), we show the time evolution of the membrane potential from the three neurons in the TDU when $R = 0.05$. For this parameter value, we see that neuron γ responds with an output spike after ≈ 54.5 msec. Also from Fig. 9(b) it is important to note the monotonic increase ($\frac{d\tau(R)}{dR} > 0$) of $\tau(R)$. This form for $\tau(R)$ with iSTDP [Eq. (5)] also results in a stable spike pattern learning mechanism for the IRU [13].

C. ISI reading unit: IRU

Using the neural circuitry for various components of the ISI reading unit, we now present two schemes for the IRU circuitry. The first utilizes a TDU with excitatory synapses and eSTDP to train on the input spike sequence. The second uses the TDU with inhibitory synapses and iSTDP to train on the input spike sequence.

1. IRU with an excitatory time-delay unit

In Fig. 10 we show the schematic diagram of the IRU built with time-delay circuitry composed of excitatory synapses. In order to understand the operation of the IRU and

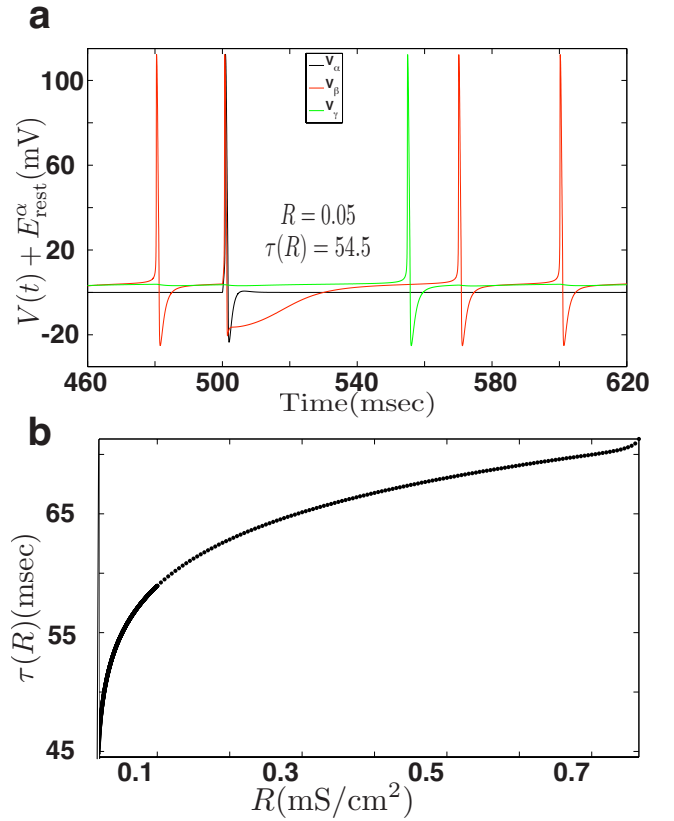


FIG. 9. (Color online) (a) We show the membrane potential of the three neurons in the TDU: neuron α (black), neuron β (red), and neuron γ (green) corresponding to input received by the TDU at time t_0 when $R = 0.05$. In this case the neuron responds with a delay of $\tau(R) = 54.5$ ms. (b) We plot the variation in the delay $\tau(R)$ produced by the TDU as a function of the parameter R . The dc currents, $I_{dc}^\alpha = 1$ mS/cm², $I_{dc}^\beta = 1.94$ mS/cm², and $I_{dc}^\gamma = 1.93$ mS/cm². The strength of inhibitory GABA_A synapse, $\gamma_{\alpha\beta} = 50$ mS/cm² and the excitatory AMPA synapses $\gamma_\alpha = g_\beta = 0.5$ mS/cm².

the mechanism of IRU training using eSTDP, we consider an input spike sequence $S = \{t_0, t_0 + T\}$ consisting of two spikes separated by an ISI T . As discussed earlier, the basic idea behind the training of the IRU is that if $|T - \tau(R)| > \delta$, where δ is the resolution for spike separation for the DU to respond with an output spike, STDP should be invoked to modulate the synaptic parameter R such that $|T - \tau(R)| \leq \delta$.

For the IRU scheme shown in Fig. 10, the input S arrives at the SSU and neuron A. Spike output from neuron A is fed into neuron α of the TDU. The first spike from the SSU at time t_0 is fed into neuron β of the TDU. An additional type I neuron γ is present in the TDU, and it serves as a relay neuron to reliably inhibit the bistable neuron β after the TDU has responded with an output spike at time $t_0 + \tau(R)$. The TDU will respond with spike at time $t_0 + \tau(R)$. The function of the neural unit \tilde{B} , which is a bistable neuron, is to prevent neuron α from responding to any spikes it receives through neuron A after it has produced a delayed spike output at time $\tau(R)$. A spike output from neuron α excites neuron \tilde{B} and moves it into its stable spiking state. It then inhibits neuron α preventing it from responding to any further input spike it receives through neuron A. Neuron α thus always responds

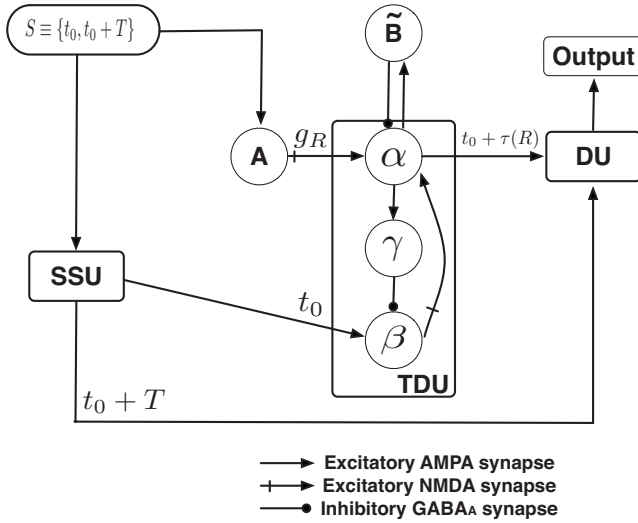


FIG. 10. Schematic diagram of the IRU comprising of the essential circuit element, the SSU, the TDU with excitatory synapse, and the DU. IRU training occurs at the synapse from neuron A (the presynaptic neuron) to neuron α (the postsynaptic neuron) depending on the synaptic strength g_R that determines the time $\tau(R)$ of the delayed spike generated by the TDU in response to an input spike it receives at time t_0 . The details of IRU training are provided in Sec. III C 2.

with a single spike output at time $\tau(R)$. The DU thus receives a single spike input from the TDU at time $\tau(R)$. The second spike from the SSU at time $t_0 + T$ is fed into the DU. If the two spikes arriving at the DU at times $t_0 + T$ from the SSU and $t_0 + \tau(R)$ from the TDU are within δ msec, the DU responds with an output spike, implying the IRU has “decoded” information embedded in ISI T . If the arrival time of the two spikes at DU is greater than δ msec, the IRU must invoke STDP to train itself on the input ISI sequence. We now explain how the IRU scheme shown in Fig. 10 can invoke eSTDP [Eq. (4)] at the synapse from neuron A (presynaptic neuron for STDP) to neuron α (postsynaptic neuron for STDP) to drive $|T - \tau(R)|$ to δ or a smaller value.

2. Training an IRU with an excitatory time-delay unit

Consider training the IRU to recognize input sequence $S = \{t_0, t_0 + T\}$ comprising of a single ISI T . Let the initial configuration of the IRU be such that $|T - \tau(R)| > \delta$ and the IRU is unable to recognize the input S and accordingly produce no output spike through the DU. In order to train the IRU to recognize this ISI input, we present the spike sequence S many times $N = 1, 2, \dots$ until $|T - \Delta\tau(R)| \leq \delta$ and the tunable synaptic strength g_R of the IRU has evolved to an asymptotic value g_{R_∞} . We consider the following two cases for training the IRU to recognize the input sequence S .

In the first case, consider the initial state of the IRU such that $|T - \tau(R)| \geq \delta$ with $\tau(R) > T$. Successful IRU training in this case requires the synaptic strength g_R to evolve with each training iteration such that $\tau(R)$ decreases eventually approaching within δ ms of T . In this case, as can be seen from the schematic diagram for the IRU in Fig. 10, neuron α fires a spike at time $t_{post} = t_0 + \tau(R)$ (postsynaptic neuron to

synapse from neuron A to neuron α) and the most effective presynaptic spike from neuron A occurs at time $t_{pre} = t_0 + T$. This implies $\Delta t = t_{post} - t_{pre} = \tau(R) - T > 0$. As a result $\Delta g(\Delta t) > 0$ and the synaptic strength g_R increases [according to the eSTDP rule in Eq. (5)] and leads to a corresponding decrease in $\tau(R)$ (since $\frac{d\tau(R)}{dR} \leq 0$) until $\tau(R)$ approaches $T + \delta$. The IRU is considered trained when the DU responds with an output spike and g_R has evolved to a final stable value g_{R_∞} corresponding to $\Delta g(\Delta t) = 0$.

The second case, when $|T - \tau(R)| \geq \delta$ with $\tau(R) < T$ is more involved. Successful IRU training in this case requires the synaptic strength g_R to evolve such that $\tau(R)$ increases approaching T from the left. In this case the most effective pre-post spike pairs for eSTDP learning are (1) presynaptic spike from neuron A at time t_0 and postsynaptic spike from neuron α at time $t_0 + \tau(R)$, corresponding to $\Delta t = \tau(R) > 0$ and (2) presynaptic spike from neuron A at time $t_0 + T$ and postsynaptic spike from neuron α at time $t_0 + \tau(R)$, corresponding to $\Delta t = \tau(R) - T < 0$. The effective change in synaptic strength per iteration of IRU training ($N = 1, 2, \dots$) is given by $g_R(N) = g_R(N-1) + \Delta G(T, \tau(R(N-1)))$, where $\Delta G(T, \tau(R)) = \Delta g(\tau(R)) + \Delta g(-|T - \tau(R)|)$. If $\Delta G(T, \tau(R(0))) < 0$, each iteration of IRU training will decrease g_R corresponding to an increase in $\tau(R)$ (since $\frac{d\tau(R)}{dR} < 0$) and as a result $\tau(R)$ approaches T . However, if the initial configuration of the IRU is such that $\Delta G(T, \tau(R(0))) > 0$, then each iteration of the IRU training will decrease $\tau(R)$ and as a result, $|T - \tau(R)|$ further increases and the IRU cannot be successfully trained to learn the ISI sequence. This implies that a successful IRU training in this situation requires the initial configuration of the IRU to be *within the basin of attraction for the stable fixed point* of the empirical eSTDP rule $\Delta g(\Delta t)$ such that $\Delta G(T, \tau(R(0))) < 0$.

In Figs. 11 and 12 we show the results from training IRU to detect ISI of $T = 100$ ms, starting from different initial configurations as discussed above. We present the spike sequence many times $N = 1, 2, \dots$ to the IRU to train the time delay to accurately reflect the input ISI sequence. The parameters of the empirical eSTDP rule are set such that the stable fixed point Δt^* corresponding to $\Delta g(\Delta t^*) = 0$ occurs at $\Delta t^* = -\delta$ ($\delta = 4$ ms) corresponding to the time resolution for coincidence spike detection by the detection unit of the IRU. This implies, with parameter values [35], $\gamma = 10^{-9}$, $\alpha_p = \alpha_D = 33.5$, $\eta = 4$, and $\beta_p \approx 2\beta_D$, we have $\beta_D = \frac{1}{3\delta} \ln(1.5) = 0.0338$. These parameter values for the eSTDP rule are within the limits of observed variability of STDP [15, 16]. The first case corresponds to $g_R(0) = 0.2$ mS/cm² corresponding to $\tau(R) = 142$ ms, so that $\tau(R) > T$. The second case corresponds to $g_R(0) = 1.63$ mS/cm² corresponding to $\tau(R) = 37.5$ ms, so that $\tau(R) < T$. This case corresponds to the initial configuration of the IRU such that the IRU is trained successfully by eSTDP to the input ISI at $T = 100$ ms. The third case corresponds to initial configuration of the IRU outside the basin for attraction of the stable fixed point Δt^* of the empirical eSTDP rule, with $g_R(0) = 1.68$ corresponding to $\tau(R) = 28.95$ ms. In this situation IRU cannot be trained to respond to input ISI $T = 100$ ms.

As can be seen from Fig. 11, starting from two different initial conditions corresponding to cases $g_R(0)$

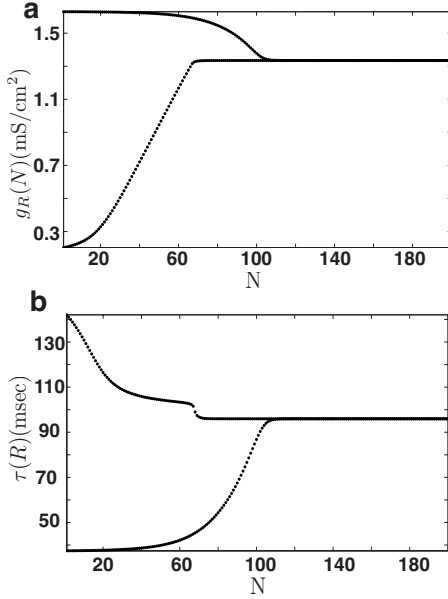


FIG. 11. Successful IRU training. (a) Evolution of the tunable synaptic strength g_R starting from two different initial configurations, as a function of the training iteration N . (b) Evolution of the time delay $\tau(R)$ produced by the IRU starting from two different initial configurations, as a function of the training iteration N .

$=0.2 \text{ mS/cm}^2$ with $\tau(R(0))=142 \text{ ms}$ such that $\tau(R) > T$, and $g_R(0)=1.63 \text{ mS/cm}^2$ with $\tau(R(0))=37.5 \text{ ms}$ such that $\tau(R) < T$, with each iteration of IRU training, the synaptic strength g_R evolves to a final stable value $g_{R_\infty} = 1.335 \text{ mS/cm}^2$ with $\Delta g(\delta)=0$ and the corresponding $\tau(R) = 96 \text{ msec}$, resulting in the IRU being successfully trained to respond with an output spike through the DU. For the third case when the initial configuration of the IRU is such that $\tau(R(0)) < T$ and $\Delta G(T, \tau(R(0))) > 0$, as we can see from Fig. 12, each training iteration of the IRU results in an increase in g_R , moving $\tau(R)$ further away from the target ISI, T , and the IRU cannot be successfully trained upon the input spike sequence S . Thus we see that there exists an upper bound on the initial strength of the synapse g_R for any given input ISI above which the IRU cannot be trained successfully. For the

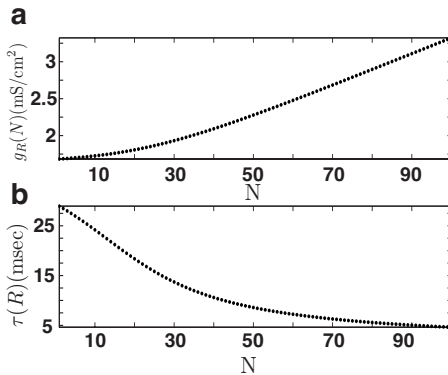


FIG. 12. Unsuccessful IRU training. (a) Evolution of the tunable synaptic strength g_R as a function of the training iteration. (b) Evolution of the time delay $\tau(R)$ produced by the IRU as a function of the training iteration.

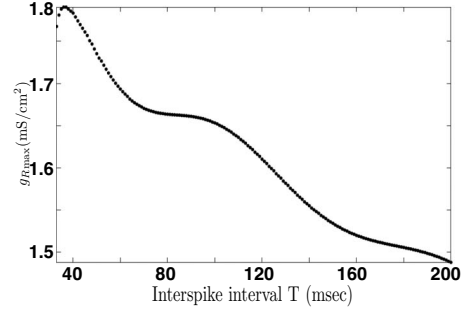


FIG. 13. The plot of the range of values for the synaptic strength $g_R \leq g_{R_{\max}}$ in the initial configuration of the IRU, in order for the IRU to be able to be trained on the input spike sequence comprising of ISI T .

case of $T=100 \text{ msec}$, the maximum initial strength $g_R(0) = 1.65 \text{ mS/cm}^2$.

We next determine the maximum strength of the synapse g_R in the initial configuration of the IRU that will result in successful IRU training for any given input ISI. For given ISI T of the input spike sequence, we determine the set $\{\vec{\tau}\}$ of all $\tau(R) < T$ that will result in $\Delta G(\tau(R), T) < 0$. This is the condition on the initial configuration of the IRU for training to recognize ISI T when the initial configuration of the IRU is such that $|T - \tau(R)| > \delta$ with $T > \tau(R)$ as discussed above. Using Fig. 6(b), we then determine the set $\{\vec{g}\}$ of synaptic strength g_R , producing the time delay $\tau(R)$ for the set $\{\vec{\tau}\}$, satisfying the condition $\Delta G(\tau(R), T) < 0$. In Fig. 13 we plot the $g_{R_{\max}} = \max(\{\vec{g}\})$ as a function T , corresponding to the maximum value of initial strength $g_R(0)$ for the excitatory synapse in the TDU, which will lead to successful IRU training for given input ISI T . We see from Fig. 13 that, for given parameters of the IRU circuitry and the eSTDP learning rule, the minimum ISI T that the IRU can train itself to recognize is $\approx 33 \text{ msec}$. For $T < 33 \text{ msec}$, no initial configuration of the IRU will result in stable IRU learning. In Fig. 14 we demonstrate an example of IRU training for this particular case, with $T=30 \text{ msec}$, and $g_R(0)=0.65 \text{ mS/cm}^2$, corresponding to

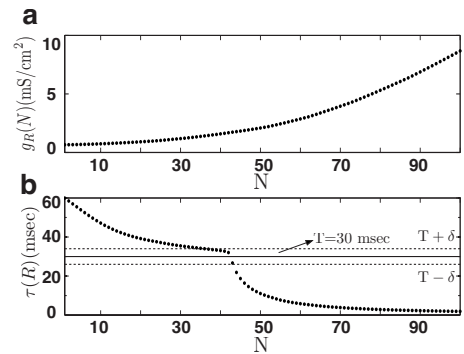


FIG. 14. Demonstration of the failure of IRU to train on the input spike sequence comprising of ISI $T=30 \text{ ms}$, for which no initial configuration of the IRU will result in stable IRU learning. Note that although with training the IRU can detect the ISI $T=30 \text{ ms}$ triggering detection by the DU, further training results in the time delay $\tau(R)$ drift away from the ISI T and the synaptic strength does not saturate to final stable configuration.

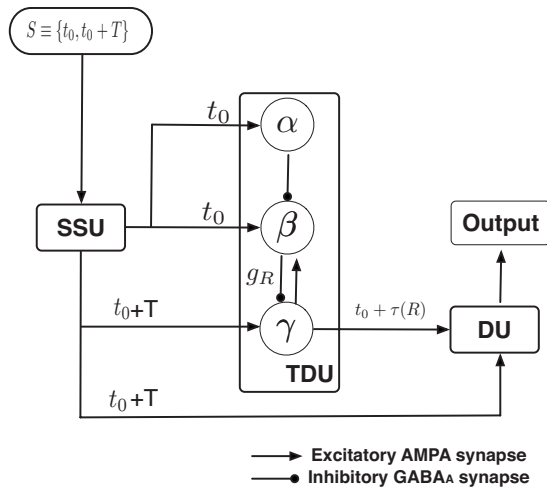


FIG. 15. Schematic diagram of the interspike IRU comprising of essential circuit elements, the SSU, the tunable TDU with inhibitory synapses, and the DU. IRU training occurs at the synapse from neuron β (the presynaptic neuron) to neuron γ (the postsynaptic neuron) within the TDU, depending on the synaptic strength g_R that determines the time $\tau(R)$ of the delayed spike generated by the TDU in response to an input spike it receives at neural units α and β at time t_0 and an input spike received by the neural unit γ at time $t_0 + T$ from the SSU. The details of IRU training are provided in Sec. III C 4.

initial configuration of the IRU resulting in $\tau(R(0)) = 60$ msec. As we can see, from Fig. 14, $\tau(R)$ decreases towards T as a function of IRU training iteration N , until $|T - \tau(R)| < \delta$, which corresponds to the IRU response through the DU. However, since the fixed point Δt^* , corresponding to $\Delta g(\Delta t^*) = 0$ is unstable, on subsequent IRU training iteration $\tau(R)$ further decreases. This is because for this case of ISI $T = 30$ msec, there exists no solution to $\Delta G(\tau(R), T = 30) < 0$. This case represents a situation when the IRU cannot successfully respond to correct ISI input after training as training does not result in the synaptic strength g_R to evolve to its asymptotic value corresponding to $\Delta g(\Delta t^*) = 0$.

3. IRU with an inhibitory time-delay unit

In Fig. 15 we show the schematic diagram of the IRU constructed using the time-delay circuitry abstracted from the AFP of the bird brain. Note the presence of excitatory synapse from neuron γ onto neuron β in the TDU component of the IRU. While the presence of this additional synapse was not required for the functioning of the TDU, it is essential for the IRU circuitry as it enables the training of the IRU through iSTDP to recognize the input spike sequence. Again, as for the case of IRU with excitatory synapses, we consider input sequence $S = \{t_0, t_0 + T\}$ comprising of single ISI T to demonstrate the functioning of the IRU. Input S arrives at the SSU as shown in Fig. 15. SSU then distributes the input spikes at time t_0 to neuron α and neuron β of the TDU. The spike from S at time $t_0 + T$ is sent by the SSU to neuron γ of the TDU and the detection unit of the IRU. Depending on the strength of synapse g_R from neuron β onto neuron γ , neuron γ responds with an output spike at time

$t_0 + \tau(R)$. It is then fed into the detection unit which again acts as a coincidence detector. Depending on the relative timing of the two spikes arriving at the DU, the DU responds with an output spike or subthreshold excitatory postsynaptic potential. An output spike from the DU represents the “decoding” of the input signal by the IRU.

If the DU of the IRU does not respond with an output spike, implying $|T - \tau(R)| > \delta$, we need a mechanism to train the IRU through its time-delay unit to adjust $|T - \tau(R)| \leq \delta$. This is done by invoking iSTDP [14] [Eq. (5)]. We now explain how the IRU is trained to recognize the input spike sequence using iSTDP.

4. Training an IRU with an inhibitory time-delay unit

We again consider training the IRU on input $S = \{t_0, t_0 + T\}$. We consider the following two cases: (1) $|T - \tau(R)| > \delta$, with $T < \tau(R)$ and (2) $|T - \tau(R)| > \delta$, with $T > \tau(R)$.

In the first situation neuron γ of the time-delay unit in the IRU fires a spike at time $t_0 + T$, which is earlier than the rebound spike at $\tau(R)$ from neuron γ . Due to the presence of the excitatory connection $\gamma \rightarrow \beta$, firing of γ at $t_0 + T$ excites neuron β , which in turn inhibits neuron γ and as a result neuron γ is prevented from producing any more spikes. The detection unit thus receives just one spike at time $t_0 + T$ and does not fire.

In this case the most effective presynaptic spike contribution to the iSTDP learning rule at the inhibitory synapse from neuron β onto neuron γ is the next spike produced by β as it resumes its oscillations after it responds to the input spike through γ at time $t_0 + T$. This occurs at time $t_0 + T + t_B$ with $t_B > 0$. This is greater than $t_0 + \tau(R)$ when neuron γ would have fired had there not been an input spike at $t_0 + T < t_0 + \tau(R)$. The iSTDP rule applied to synapse from $\beta \rightarrow \gamma$ thus sees $\Delta t = (t_0 + T) - (t_0 + T + t_B) < 0$. This leads to a decrease in g_R and as shown in Fig. 9(b), a decrease in $\tau(R)$ (since $\frac{d\tau(R)}{dR} > 0$). The decrease in $\tau(R)$ continues until $|T - \tau(R)| \leq \delta$ and the DU receives two spikes within δ msec, to respond with an output spike and the synaptic strength has evolved to a final asymptotic value.

In the second situation, when $T > \tau(R)$ and $|T - \tau(R)| > \delta$, the learning rule must be invoked to increase $\tau(R)$. Neuron γ produces a spike at time $t_0 + \tau(R)$ resulting in a spike response in neuron β at time $t_0 + \tau(R) + \epsilon$, where ϵ corresponds to the synaptic delay, which is due to the excitatory feedback from neuron γ onto neuron β . This excitation of neuron β is presynaptic to the $\beta \rightarrow \gamma$ inhibitory coupling and is identified with t_{pre} in the STDP rule. Neuron γ again receives excitatory input at time $t_0 + T$. This is postsynaptic to the $\beta \rightarrow \gamma$ inhibitory coupling and we set $t_{post} = t_0 + T$ so that $\Delta t = T - \tau(R)$. This combination of spiking activity in neurons β and γ results in an increase in the $\beta \rightarrow \gamma$ inhibitory synaptic connection g_R . Since $\frac{d\tau(R)}{dR} > 0$, $\tau(R)$ increases, approaching T from below. This learning process continues until $|T - \tau(R)| < \delta$ when the detection unit fires and again g_R reaches a final steady state value.

The IRU is trained as presented above by invoking the iSTDP training rule as follows:

$$\Delta g_R = \frac{g_s}{g_{norm}} \sum_j \alpha^\beta \Delta t_j |\Delta t_j|^{\beta-1} \exp(-\alpha |\Delta t_j|), \quad (6)$$

with $g_s=0.01$ and $g_{norm}=\beta^\beta e^{-\beta}$. The parameters $\alpha=0.54$, $\beta=3.0$ when $\Delta t>0$ and $\alpha=0.25$, $\beta=5.0$ when $\Delta t\leq 0$. Although the choice of these parameter values differ from the symmetric iSTDP learning rule shown in Fig. 1(b), the essential properties of the iSTDP rule are preserved, i.e., $\Delta g(\Delta t)>0$ for $\Delta t>0$, $\Delta g(\Delta t)<0$ for $\Delta t<0$, and $\Delta g(\Delta t)\approx 0$ for $\Delta t\approx 0$ and for the chosen values for the learning rule the IRU can be trained over the entire range of $\tau(R)$ values that can be generated by the three neuron TDU.

$\Delta t_j=T_\gamma-T_{\beta_j}$ when we have one postsynaptic spike in neuron γ at time T_γ as in the case when $T<\tau(R)$, with T_{β_j} representing the presynaptic spike times of neuron β . In the situation when there are two postsynaptic spikes in neuron γ at times T_{γ_1} and T_{γ_2} , such that $T_{\gamma_1}<T_{\gamma_2}$ as in the case when $T>\tau(R)$, we compute Δt_j as

$$\Delta t_j = \begin{cases} T_{\gamma_1} - T_{\beta_j}, & T_{\beta_j} \leq T_{\gamma_1} \\ T_{\gamma_2} - T_{\beta_j}, & T_{\beta_j} > T_{\gamma_2} \\ (T_{\gamma_1} - T_{\beta_j}) + (T_{\gamma_2} - T_{\beta_j}), & T_{\gamma_1} < T_{\beta_j} \leq T_{\gamma_2}. \end{cases}$$

The contribution of multiple spike pairs in the iSTDP learning above is considered additively [40]. Additive rules for multiple spike pairs have also been considered in earlier works [41,42]. Note that in this case, the nearest neighbor spike-pair interaction for iSTDP learning will not modulate the synapse g_R , due to the presence of the excitatory connection from neuron γ to neuron β , since every time neuron γ fires, neuron β will fire within the time scale of the AMPA synapse between the two neurons and the iSTDP rule from Eq. (5) implies zero in Δg over this time scale.

We present the spike sequence many times $N=0,1,2,\dots$ to the IRU to train the time delays to accurately reflect the individual ISIs in the sequence. In Fig. 16 we present results from training the IRU starting from two initial configurations tuned to detect an ISI of $T=60$ msec. In the first configuration, presented in Fig. 16(a), IRU has $g_R(0)=0.4$, corresponding to $\tau(R)\approx 67$ msec, so that $T<\tau(R)$. Since there is an excitatory synapse from neuron γ to neuron β , in this case, neuron γ does not produce a delayed spike at $\tau(R)$ and the detection unit only receives a single spike output. In Fig. 16(a) (bottom), we show the time of output from neuron γ , which in this case is at time $t_0+T+\epsilon$. This case corresponds to a decrease in g_R with each training of the IRU as discussed above, until eventually $\tau(R)<T$. At that point the significant contribution to synaptic rule occurs through Eq. (7), and the synaptic strength g_R increases until again $T>\tau(R)$ and the TDU produces one spike output. This cycle continues as can be seen from Fig. 16(a). The synaptic strength evolves to a final asymptotic state with $|T-\tau(R)|\leq\delta$ and $\tau(R)<T$, such that the DU receives two spikes within δ msec, for it to respond with a spike output. Subsequent presentation of the same spike sequence will successfully elicit a spike response from the IRU, corresponding to the ‘‘decoding’’ of information embedded in the input spike sequence.

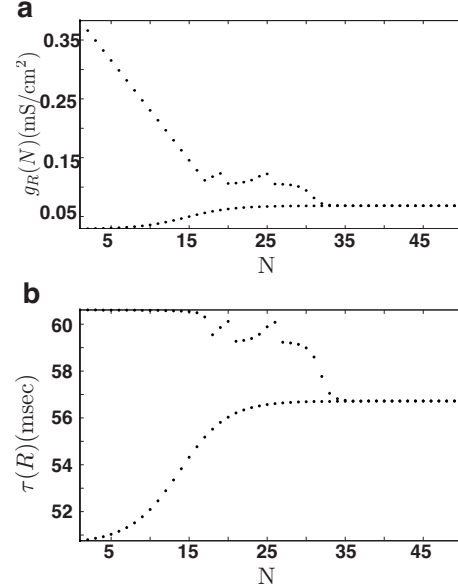


FIG. 16. Successful IRU training. (a) Evolution of the tunable synaptic strength g_R starting from two different initial configurations, as a function of the training iteration. (b) Evolution of the time delay $\tau(R)$ produced by the IRU starting from two different initial configurations, as a function of the training iteration.

For the second case, we have $g_R(0)=0.029$ leading to $\tau(R)\approx 50.5$ msec, so $T<\tau(R)$. In this case, each training of the IRU results in an increase in synaptic strength g_R until, again $|T-\tau(R)|\leq\delta$ and the IRU is considered trained when g_R reaches a final asymptotic value.

Successful training of the IRU with inhibitory synapses to recognize input spike sequence is limited to the bandwidth of the time-delay component of the IRU. We observe that for biologically realistic parameter values for the neuron model and the synaptic strength, the bandwidth is limited to a range of $\approx 20-30$ msec. The IRU will fail to train on any ISI outside the range of time delays permitted by the time-delay circuitry. In addition the IRU training is more susceptible to the presence of an extraneous spike in neuron β of the TDU, as the spike output from neuron γ is measured relative to the spiking time of neuron β in the TDU.

Finally, in Fig. 17 we test the robustness of both IRU configurations (Figs. 10 and 15) to train upon input ISI in the presence of random jitter. During each training iteration, the IRU receives the input spike sequence $S=\{t_0, t_0+T\}$ with ISI T , modulated by a random jitter of ± 2 msec, drawn from a uniform distribution. The IRU with an excitatory time-delay unit was trained upon ISI $T=100$ msec, similar to the configuration considered in Fig. 11 and the IRU with inhibitory synapse was trained upon an ISI $T=60$ msec, similar to the configuration considered in Fig. 16. For this level of noise in the ISI during the training, both IRUs are able to successfully train to recognize the input spike sequence. It should be noted that for the successful convergence to a final asymptotic state, the maximum jitter in the training sequence can be $\pm\delta$ msec. If the jitter is greater than $\pm\delta$ then by chance $|T-\tau(R)|>\delta$ and the IRU cannot converge to a final steady state.

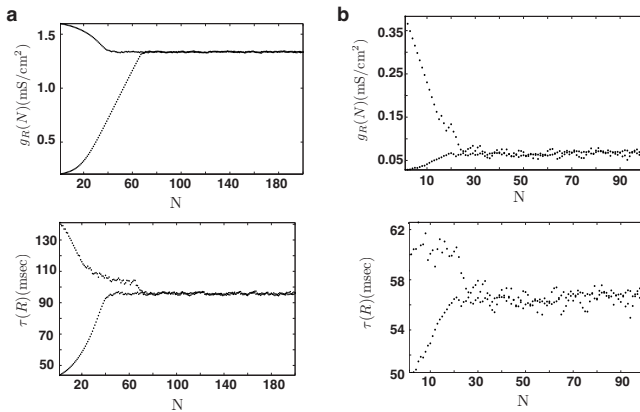


FIG. 17. (a) Training IRU with a time-delay unit consisting of excitatory synapse to detect $ISI\ T=100\ \text{ms}$ in the presence of noise. (b) Training the IRU with a time-delay unit consisting of inhibitory synapse to detect $ISI\ T=60\ \text{ms}$ in the presence of noise. In both cases (top) evolution of synaptic strength $g_R(N)$ and (bottom) evolution of the time delay $\tau(R)$ starting from two different initial configurations.

IV. DISCUSSION

We constructed neural circuits for temporal spike pattern recognition comprised of biologically motivated neurons and biologically motivated synaptic connections. We refer to such neural circuitry as the IRU. We begin by describing the general architecture for the IRU circuitry assigned the task of spike pattern recognition. We then provide a particular circuit implementation for the input component of the IRU, the SSU, and the output of the IRU through the DU. We then describe two possible architectures for the TDU circuitry of the IRU, based on its ability to produce a delayed spike output through the modulation of the excitatory and inhibitory synapse, respectively. While the TDU with inhibitory synapse was derived from anatomical observation of the AFP in songbirds, the TDU with excitatory synapse was constructed as a biologically feasible implementation of the “concept” TDU, comprised of a single neuron. The TDU components in the IRU are modulated through experimentally observed spike timing dependent plasticity rules for excitatory and inhibitory synapses in order for the IRU to respond to a spike sequence of interest, until they match the ISI within certain precision, taken here to be $\delta=4\ \text{ms}$.

The construction of the two IRU circuits to read ISIs in the chosen sequence are quite general and are not solely connected with the observations of the AFP circuitry in songbirds that motivated the construction. It could be, though we do not have anatomical or electrophysiological evidence for this at this time, that such circuitry could be used generally to recognize the specific ISI sequences produced by sensory systems in response to environmental stimuli. It seems clear that some circuit of this kind, whether or not it is the one we construct here, may well be utilized by animals for recognition of important sensory inputs [43–45]. Those inputs are transformed by the sensory system into spike sequences, and in a situation when all the spikes produced are identical, all the information is represented in the spike sequence. Reading those sequences in premotor or decision processing is required for various functional activities.

We gave examples of the training of the two IRU networks using both inhibitory and excitatory synaptic plasticity rules. While the implementation of the IRU with time-delay circuitry motivated from songbirds was explored earlier [13], here we describe in detail the abstraction of the TDU from the songbird AFP circuitry. We describe in detail the condition under which IRU with excitatory synapse can be trained to recognize an input ISI sequence and demonstrate through examples when the IRU will fail to recognize an input ISI sequence.

We have made two important assumptions in the plasticity update rules used in the training of the IRUs [46]. Only neighboring spike pairs between the pre and postsynaptic neurons were considered for STDP and we assumed that the effect of STDP modulation sums linearly. The construction of the IRUs was such that the most significant contribution to the modulation in the synapse occurs through the neighboring spike pairs. Multispike pair interactions have been considered earlier in STDP through natural spike trains [40]. It would be interesting to consider a differential equation form for the STDP rules [35] which have the intrinsic mechanism to account for the effects of multispike interactions and see how it influences the performance of the IRU scheme. The second key assumption that we have made in our consideration of the STDP dependent update of synaptic strength is that the update happens instantaneously, thereby we ignore the delay of several minutes that exists between the pairing of pre- and postsynaptic spikes and the induction of synaptic changes. Our assumption implies that the time scales of synaptic modification are much faster than the spiking rate of neurons, which is contrary to experimental observations, however, the mere introduction of delay in the synaptic update rule has no consequence for our results. We tested this assumption by decreasing the intensity of the STDP update rule [γ , in Eq. (4) and g_s in Eq. (6)] such that the increment in the synaptic strength during each training session is much smaller. Although this resulted in an increase in the number of training sessions for the IRU the overall results were the same and the IRU was trained to recognize the input spike sequence.

To examine the generality of our construction of an IRU we have used both conductance based Hodgkin-Huxley model neurons and phenomenological quadratic integrate and fire neurons at the nodes of our networks for both IRU implementations (results for the quadratic integrate and fire model not shown) using the same synaptic currents connecting the neurons. While the results differ in details, each IRU shows much the same learning properties, leading us to be confident that a construct such as an IRU can be a property of many different specific realizations of neurons at the nodes of the time delay and IRU circuits as long as the pattern of inhibition and excitation essential to the function of the circuit is maintained.

Our analysis does not address the response of an IRU to a desired ISI sequence when it is embedded in environments with many extraneous spikes, and it does not address the reliability of the synaptic connections as a potential source of error in reading ISI sequences. It may be that the actual biological environments in which IRUs operate, assuming them to be present, require a statistical measure of detection efficacy.

Finally, we wish to note that although our motivation for the IRU construction was derived from the observed neural circuitry for song learning in songbirds, to our knowledge there is no anatomical evidence at this time in any biological system of the IRU implementation we have developed here for the specific task of temporal spike pattern recognition. The task of decoding sensory information embedded in spike patterns produced by the brain is vitally important for biological function and it may well be that IRU circuitry would be one way for the neural system to learn to respond to correct sensory inputs.

ACKNOWLEDGMENTS

This work was performed under the sponsorship of the Office of Naval Research (ONR Grant No. N00014-02-1-1019) and the National Institute of Health Collaborative Research in Computational Neuroscience program (Grant No. 1R01EB004752). W.L.D. was partially funded from the J. Crayton Pruitt Family Endowment funds. S.S.T. was partially funded through the Epilepsy Foundation of America. H.D.I.A. is partially supported by the NSF sponsored Center for Theoretical Biological Physics at UCSD and by a contract with the Office of Naval Research, MURI grant (ONR Grant No. N00014-07-1-0741)

APPENDIX: LINEAR MAP FOR LEARNING RULE

We want to emphasize that successful IRU training is dependent on two key properties exhibited by the IRU.

(1) The monotonic increasing or decreasing relationship of the time delay $\tau(R)$ produced by the time-delay units with inhibitory or excitatory synaptic modulation.

(2) The spike timing dependent plasticity rule governing the evolution of synaptic strength dependent on the relative timing of the pre- or postsynaptic spikes.

In order to explore the generality of IRU learning, dependent on the two key properties presented above, in this section we consider an approximation of the learning rule for the evolution of the inhibitory synapse, and the delay produced by each delay unit as a function of the strength of inhibitory connection from $\beta \rightarrow \gamma$, as shown in Figs. 18(a) and 18(b). We compute an analytical expression for the number of training sequence steps required for a delay unit (for IRU with inhibitory synapses) to detect a spike within δ ms resolution of an ISI. The approximation shown in Figs. 18(a) and 18(b) results in the following:

$$\frac{\Delta g_I}{g_{I_0}} = b\Delta t \quad (|\Delta t| \leq A) = -b\Delta t + 2Ab \quad (A < |\Delta t| \leq 2A)$$

$$= 0 \quad (|\Delta t| > 2A), \quad (\text{A1})$$

with $\tau = ag_I + c$ ($g_L \leq g_I \leq g_U$) and $\tau = 0$ ($g_I < g_L$) and $\tau = \tau(g_U)$ ($g_I > g_U$). The fact that $\Delta g = 0$ for $|\Delta t| > 2A$ implies that, learning will occur only for Δt in the range of $\pm 2A$ ms, or in the map $f(g_I(N))$ the allowed variation in $g_I(N)$ is from $(T-c-2A)/a$ to $(T-c+2A)/a$. Depending on the initial inhibitory synaptic strength of $g_I(0) = g_0$, with the above linear learning rule, the number of steps for the delay unit to set its

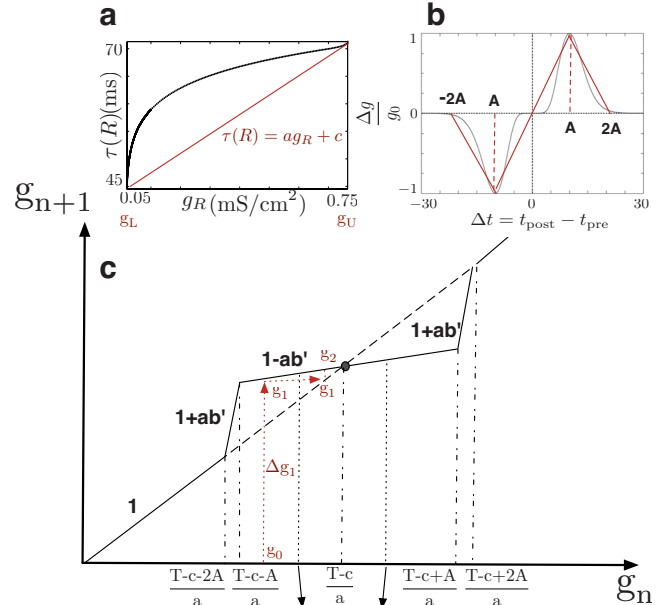


FIG. 18. (Color online) (a) Linear approximation for the delay produced by the time-delay unit with inhibitory synapse. (b) Linear approximation for the iSTDP learning rule. (c) Linear map for the evolution of the inhibitory synaptic strength as a function of the IRU training iteration number. Sample trajectory of the evolution of inhibitory synaptic strength following the linear iSTDP learning rule is shown by a dotted red line.

delay output within δ ms of actual ISI time that it needs to detect, $N(\delta)$, can be obtained as follows.

The trivial case of the initial condition being within the δ window of actual ISI, results in $N(\delta) = 0$. In the situation when $|\Delta t| \leq A$, the number of training iterations required for learning is given by $N(\delta) = 1 + n_1$, where n_1 can be computed as follows. We begin in the region $\Delta t = T - \tau_0 \leq A$, which corresponds to initial inhibitory synaptic strength lying in the interval $(T-c-A)/a \leq g_I(0) \leq (T-c-\delta)/a$. At each iteration step i , as shown in the example path in Fig. 18(c), $g_I(i)$, increments by amount, $\Delta g_I(i)/(1-ab')$, where $b' = bg_{I_0}$. The total number of integer steps required for $g_I(0) = g_0$, to evolve to within the δ ms window of T , is then given by

$$n_1 = \left\lceil \frac{\ln\left(\frac{\delta}{(|T-\tau_0|)}\right)}{\ln(1-ab')} \right\rceil, \quad (\text{A2})$$

where $\tau_0 = ag_0 + c$, and $[x]$ is the largest integer less than or equal to x .

It is important to note the factor of b' appearing in the denominator of the above equation. In the scheme of learning rule we have used in the main calculations, as $\Delta t \rightarrow 0$, b' , which represents the slope of the learning curve approaches 0, and as we can see from above, theoretically the exact convergence of learning, i.e., $\Delta t = 0$ requires an infinity of training steps.

In the situation when the initial condition is such that $A < |\Delta t| < 2A$, the number of training iterations required is given by $N(\delta) = 2 + n_1 + n_2$, where

$$n_1 = \left\lceil \frac{\ln\left(\frac{A}{|2A + \tau_0 - T|}\right)}{\ln(1 + ab')} \right\rceil,$$

$$n_2 = \left\lceil \frac{\ln\left(\frac{\delta}{|(T - c) - a\tilde{g}|}\right)}{\ln(1 - ab')} \right\rceil,$$

$$\tilde{g} = g_0(1 + ab')^{n_1+1} + \frac{((1 + ab')^{n_1+1} - 1)(2A - (T - c))}{a}. \quad (\text{A3})$$

Linear fit to the learning rule used in the main text, which is abstracted from empirical fit to entorhinal cortex data, gives $A = 5$ ms, $b' = 0.02$ ms⁻¹ and the linear $\tau(g)$ curve implies $a = 0.9$ ms, $c = 42.58$ ms, $g_L = 0.75$, and $g_U = 22.0$. In this approximation the maximum number of steps will correspond to beginning with the Δt error of $\pm 2A = 10$ ms. For a particular case of $T = 60$ ms, and beginning with $\tau_0 = 51$ ms, giving $\Delta t = 9$ ms, and taking $\delta = 1$ ms, solving the above equation gives $N = 179$, as the total number of training cycles for the delay unit to learn.

We thus see that for IRU with inhibitory synapses, resulting in a monotonic increasing relationship of the time delay $\tau(R)$ with respect to the synaptic strength g_R , the IRU can be trained in a finite number of training iterations using the iSTDP rule that satisfies the two key properties of $\Delta g > 0$ when $\Delta t > 0$ and $\Delta g < 0$ when $\Delta t < 0$.

-
- [1] R. M. Fano, *Transmission of Information, A Statistical Theory of Communications* (MIT Press, New York, 1961).
- [2] E. Aarabzadeh, S. Panzeri, and M. E. Diamond, *J. Neurosci.* **24**, 6011 (2004).
- [3] C. Welker, *J. Comp. Neurol.* **166**, 173 (1976).
- [4] G. Buracas, A. M. Zador, M. DeWeese, and T. Albright, *Neuron* **9**, 59 (1998).
- [5] Y. Sugase, S. Yamane, S. Ueno, and K. Kawano, *Nature (London)* **400**, 869 (1999).
- [6] M. Coleman and R. Mooney, *J. Neurosci.* **24**, 7251 (2004).
- [7] M. Lewicki and B. Arthur, *J. Neurosci.* **16**, 6897 (1996).
- [8] D. Margoliash, *J. Neurosci.* **3**, 1039 (1983).
- [9] D. Margoliash, *J. Neurosci.* **6**, 1643 (1986).
- [10] J. A. Cardin, J. N. Raskin, and M. F. Schmidt, *J. Neurophysiol.* **95**, 1158 (2006).
- [11] C. E. Carr, *Annu. Rev. Neurosci.* **16**, 223 (1993).
- [12] P. Janata and D. Margoliash, *J. Neurosci.* **19**, 5108 (1999).
- [13] H. D. I. Abarbanel and S. S. Talathi, *Phys. Rev. Lett.* **96**, 148104 (2006).
- [14] J. Haas, T. Nowotny, and H. Abarbanel, *J. Neurophysiol.* **96**, 3305 (2006).
- [15] G. Bi and Mu-ming, *J. Neurosci.* **18**, 10464 (1998).
- [16] G. Bi and M. Poo, *Annu. Rev. Neurosci.* **24**, 139 (2001).
- [17] D. Buonomano and U. R. Karmarkar, *Neuroscientist* **8**, 42 (2002).
- [18] R. Ivry, *Curr. Opin. Neurobiol.* **6**, 851 (1996).
- [19] M. D. Mauk and D. Buonomano, *Annu. Rev. Neurosci.* **27**, 307 (2004).
- [20] D. Buonomano, *J. Neurosci.* **20**, 1129 (2000).
- [21] C. E. Carr and M. Konishi, *J. Neurosci.* **10**, 3227 (1990).
- [22] E. Knudsen and M. Konishi, *J. Neurophysiol.* **41**, 870 (1996).
- [23] C. Koppel, *J. Neurosci.* **17**, 3312 (1997).
- [24] D. B. Forger and C. Peskin, *Proc. Natl. Acad. Sci. U.S.A.* **100**, 14806 (2003).
- [25] D. B. Forger and C. Peskin, *J. Theor. Biol.* **230**, 533 (2004).
- [26] R. R. Kimpo, F. E. Theunissen, and A. J. Doupe, *J. Neurosci.* **23**, 5750 (2003).
- [27] H. D. I. Abarbanel, S. S. Talathi, G. B. Mindlin, M. I. Rabinovich, and L. Gibb, *Phys. Rev. E* **70**, 051911 (2004).
- [28] D. J. Perkel, *A Basal Ganglia Circuit Essential for Vocal Learning* (2002); URL <http://mbi.osu.edu/2002/ws6materials/perkel.ppt>
- [29] D. J. Perkel, *Ann. N.Y. Acad. Sci.* **1016**, 736 (2004).
- [30] B. Ermentrout, *Neural Comput.* **8**, 979 (1996).
- [31] J. Crawford, *Rev. Mod. Phys.* **63**, 991 (1991).
- [32] E. Izhikevich, *Dynamical Systems in Neuroscience* (MIT Press, Cambridge, Massachusetts, 2007).
- [33] J. Magee and D. Johnston, *Science* **275**, 209 (1997).
- [34] H. Markram, J. Lubke, M. Frotscher, and B. Sakmann, *Science* **275**, 213 (1997).
- [35] H. D. I. Abarbanel, R. Huerta, and M. Rabinovich, *Proc. Natl. Acad. Sci. U.S.A.* **99**, 10132 (2002).
- [36] M. S. Brainard and A. J. Doupe, *Nature (London)* **417**, 351 (2002).
- [37] E. A. Brenowitz, D. Margoliash, and K. W. Nordeen, *J. Neurobiol.* **33**, 495 (1997).
- [38] M. A. Farries, L. Ding, and D. J. Perkel, *J. Comp. Neurol.* **484**, 93 (2005).
- [39] M. A. Farries and D. J. Perkel, *J. Neurosci.* **22**, 3776 (2002).
- [40] R. Froemke and Y. Dan, *Nature (London)* **416**, 433 (2002).
- [41] R. Kempster, W. Gerstner, and J. L. van Hemmen, *Phys. Rev. E* **59**, 4498 (1999).
- [42] P. Robert, *J. Comput. Neurosci.* **7**, 235 (1999).
- [43] J. Hopfield and C. Brody, *Proc. Natl. Acad. Sci. U.S.A.* **98**, 1282 (2001).
- [44] W. Maass, *Neural Comput.* **14**, 2531 (2002).
- [45] R. Gutig and H. Sompolinsky, *Nat. Neurosci.* **9**, 420 (2006).
- [46] S. S. Talathi, D.-U. Hwang, and W. Ditto, *J. Comput. Neurosci.* **25**, 262 (2008).